CrossMark

REVIEW

# Mesenchymal stem cell cultivation in electrospun scaffolds: mechanistic modeling for tissue engineering

Ágata Paim[1] · Isabel C. Tessaro[1] ·
Nilo S. M. Cardozo[1] · Patricia Pranke[2,3]

**Abstract** Tissue engineering is a multidisciplinary field of research in which the cells, biomaterials, and processes can be optimized to develop a tissue substitute. Three-dimensional (3D) architectural features from electrospun scaffolds, such as porosity, tortuosity, fiber diameter, pore size, and interconnectivity have a great impact on cell behavior. Regarding tissue development in vitro, culture conditions such as pH, osmolality, temperature, nutrient, and metabolite concentrations dictate cell viability inside the constructs. The effect of different electrospun scaffold properties, bioreactor designs, mesenchymal stem cell culture parameters, and seeding techniques on cell behavior can be studied individually or combined with phenomenological modeling techniques. This work reviews the main culture and scaffold factors that affect tissue development in vitro regarding the culture of cells inside 3D matrices. The mathematical modeling of the relationship between these factors and cell behavior inside 3D constructs has also been critically reviewed, focusing on mesenchymal stem cell culture in electrospun scaffolds.

**Keywords** Stem cells · Tissue development · Electrospun scaffolds · Phenomenological modeling

✉ Ágata Paim
  agata@enq.ufrgs.br

[1] Department of Chemical Engineering, Universidade Federal do Rio Grande do Sul (UFRGS), R. Eng. Luis Englert, s/n, Porto Alegre, Rio Grande do Sul 90040-040, Brazil

[2] Faculty of Pharmacy, Universidade Federal do Rio Grande do Sul (UFRGS), Av. Ipiranga, 2752, Porto Alegre, Rio Grande do Sul 90610-000, Brazil

[3] Stem Cell Research Institute, Porto Alegre, Rio Grande do Sul 90020-010, Brazil

🖄 Springer

# 1 Introduction

Tissue engineering is a potential alternative for tissue transplants and applies basic principles of engineering to restore, preserve, and/or enhance tissue function [1]. In tissue engineering, biomaterials can be engineered to produce scaffolds that mimic the extracellular matrix environment, taking into consideration appropriate architecture, biodegradability, biocompatibility, and mechanical properties [2].

There are commercial devices available for tissue engineering but their high cost can impair the treatment of large tissue damage [3]. In addition, according to the regulated commercial products presented by Place, Evans, and Stevens [4], 87% of these products use animal-derived materials (e.g., porcine, bovine, equine or rat collagen, or decellularized tissue); 37% present nutrient diffusion limitations (products in sheet form) and only 25% contain cells (e.g., MACI, Hyalograft C autograft and CaRes contain chondrocytes, and TransCyte, Apligraf, and Dermagraft contain human fibroblasts). In order to reduce the risks of adverse immunological response and animal component contamination and pathogen transmission, many efforts are being made to develop low-cost xeno-free (with no animal-derived components) devices [5, 6].

The combination of different scaffold fabrication techniques (freeze-thawing [7], knitting [8], braiding [9], fused deposition modeling [10]) and biomaterials (natural [11], synthetic [7, 9, 10], and hybrid [8]) have been explored in several commercial products. After an initial focus on the development of skin substitutes for burn treatment, the engineering and availability of devices for other tissue types, such as bone [12], cartilage [13], vascular [14], and nerve [15], have become possible.

Many tissue-engineering strategies are based on the culture of autologous cells in scaffolds: BioSeed-C, CaRes, Hyalograft C autograft, MACI, Neo-bladder, and VascuGel [4, 13]. However, autologous cell sampling requires an invasive procedure and may not provide a sufficient cell number for expansion or transplant techniques [16, 17]. Meanwhile, mesenchymal stem cells (MSCs) are a potential alternative for tissue regeneration because of their differentiation potential and highly proliferative and immune-privileged characteristics [17–20].

However, the success of cell culture in three-dimensional scaffolds requires adequate culture conditions. Aside from cell viability, the culture parameters should be able to provide chemical, electrical, and mechanical stimuli to induce specific cell responses and generate functional tissue [21, 22]. In this review, the main scaffold architecture and culture conditions features affecting tissue development in vitro are discussed with an emphasis on the culture of mesenchymal stem cells in electrospun scaffolds. Furthermore, tissue engineering applications of several bioreactor systems and seeding techniques are synthesized. Regarding these process variables, mechanistic modeling applications in tissue engineering are reviewed.

# 2 Scaffolds

Several types of biomaterials can be used as scaffolds in tissue engineering, such as films, beads, and porous three-dimensional matrices (Fig. 1).

Films can be used as bi-dimensional (2D) scaffolds and, along with MSCs, can be employed to develop substitutes for vascular tissue [23]. However, 2D scaffolds are unable to support in vitro cell growth and organization in a tissue-like structure because in vivo
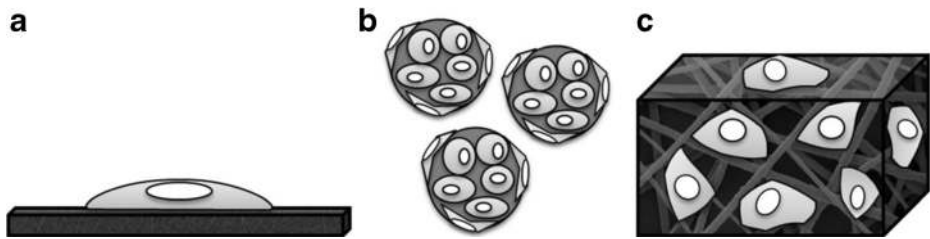
Fig. 1 Types of structures for cell attachment and culture: film (**a**), beads (**b**), and porous scaffold (**c**)

the extra-cellular matrix (ECM) provides a three-dimensional (3D) microenvironment for the cells [24]. While 2D cultures are not affected by biophysical properties of the matrix, 3D scaffolds provide physical and chemical signals to guide tissue development [25]. In this context, the interaction of MSCs with biomaterials can be investigated using a 2D platform to determine suitable models for further investigation in 3D structures for bone engineering [26]. In addition, porous films seeded with cells can be stacked to engineer a 3D corneal substitute [27].

3D scaffolds can be fabricated in the form of beads or blocks with a defined shape [28]. Beads are usually alginate [29], collagen [30], calcium phosphate, e.g., tricalcium phosphate [29], and polymer [31] based spherical structures designed for further molding into a 3D defined shape [30–32] or for injection for minimally invasive treatment to repair bone defects [29]. Beads and injectable hydrogels have also been used as soft tissue fillers in adipose [33] and cartilage [34] tissue engineering. Hydrogels are composed of crosslinked hydrophilic polymer chains [35] and can be produced in specific shapes other than microspheres [36]. However, their application is usually limited to soft tissue due to their poor mechanical properties [37].

MSCs have been cultivated in ceramic [38], metallic [39], and polymeric [40] porous 3D solid scaffolds to develop substitutes for load-bearing tissue. However, metals are non-resorbable [39] and ceramics present low fracture toughness and brittleness [41]. On the other hand, synthetic biodegradable polymers have been used to develop 3D porous scaffolds for hard [42] and soft [43] tissue engineering due to their adequate mechanical properties and degradability.

The use of biodegradable polymer blends in tissue engineering allows for adjustment of the scaffold performance in terms of biocompatibility, processability, mechanical resistance, and degradation rate [44]. Aliphatic polyesters, such as polycaprolactone (PCL), polylactic acid (PLA), polyglycolic acid (PGA), and their copolymers degrade mostly by the hydrolysis of the ester bonds in acid monomers that can be removed from the body by metabolic routes, characterizing them as bioresorbable materials [45, 46]. However, degradation byproducts can affect the medium acidity, and consequently, cell viability, migration, and angiogenesis [47]. The local accumulation of these byproducts can be avoided with a perfusion culture system, which can also reduce the polymer degradation rate [48].

The fabrication process can determine the architecture and mechanical properties of the scaffold. The more common techniques to produce polymeric porous 3D structures for tissue engineering are gas foaming, fiber extrusion and bonding, electrospinning, solid free-form fabrication, 3D printing, phase separation, solvent casting/particulate leaching, freeze-drying, and emulsion freeze-drying [43]. However, interconnectivity and pore size and shape are not always controllable with most of these methods [49].

According to Pulikkot et al. [50], when compared to non-porous and microporous polycaprolactone scaffolds, microfibrous matrices enhanced cell proliferation as a result of the higher surface roughness and area available for cell adhesion. Electrospinning is a technique capable of producing micro and nanofibrous scaffolds with interesting characteristics for tissue engineering, allowing for the use of a wide range of polymers [51]. The self-organization process of the fibers is induced by electrostatic repulsion forces (Fig. 2), assigning to the technique high versatility in terms of morphology, surface topology, and fiber property control [52]. The stability of the fiber-formation process can be complex, as it is influenced by the spinning solution properties, electrospinning parameters, environmental conditions, and interactions among these variables [53, 54]. Besides this, the electrospinning technique is characterized by a low productivity rate [54, 55] and tendency to produce thin scaffolds with small pores. The latter is a significant drawback in the production of 3D tissues because it can hinder cell infiltration and the manufacture of large structures [56, 57].

Electrospun scaffolds have high packing density (ratio of surface area to total volume), highly interconnected pore networks, and fibers with diameters similar to the dimensions of the extracellular matrix protein network [58]. In addition, electrospinning enables the fiber thickness to be controlled through the manipulation of process variables, allowing for the study of the impact of the porous matrix spatial architecture on cell behavior [59].

Due to their unique features, the use of nanofibrous electrospun scaffolds in tissue engineering is expanding rapidly. Polycaprolactone/collagen/hydroxyapatite (PCL/col./HA) [60], fibrinogen/polydioxanone (Fg/PDO) [61], and polycaprolactone/polylactic acid (PCL/PLA) [62] nanofibrous electrospun scaffolds have been shown to promote bone regeneration in vitro when seeded with human MSCs. In diabetic animal models, 3D poly(lactic acid-co-glycolic acid) (PLGA) electrospun scaffolds have been used for chronic wound repair [63], while poly-L-lactide acid (PLLA) electrospun devices have been able to improve insulin
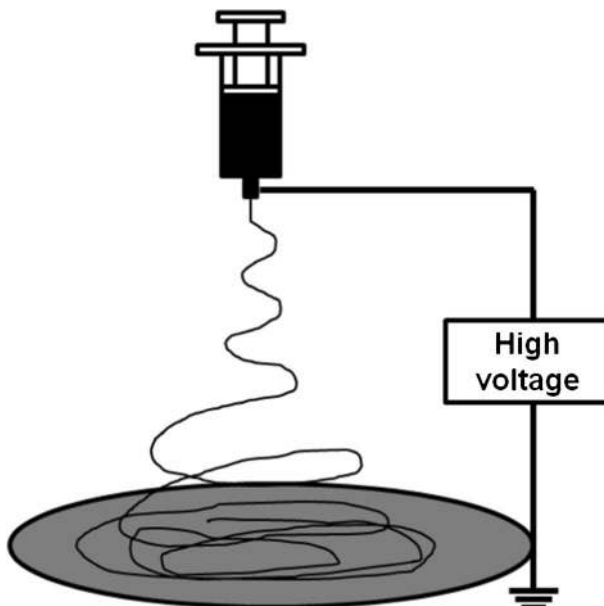


**Fig. 2** Electrospinning setup scheme

secretion [64]. Polymeric nanofibrous electrospun scaffolds have also been applied in clinical trials for the treatment of cutaneous leishmaniasis [65], diabetic foot ulcers [66], and for human pelvic floor reconstruction [67].

## 3 Scaffold architecture impact on cell behavior

The chemical nature and architecture of a 3D scaffold can affect cell proliferation and differentiation due to its importance in cell adhesion and migration and in mass transport within the matrix [68].

Scaffold porosity has a direct impact on the supply of nutrients to the cells, metabolite dispersion, pH local stability, and cell signaling [69]. Higher porosities are known to support larger cell densities and to enhance cell proliferation and differentiation [70, 71]. In addition, scaffolds with higher porosity often present higher permeability and cell infiltration [72, 73]. However, a larger void fraction can lead to poor mechanical resistance [72]. Thus, the biomaterial porosity must be optimized to allow for cell interaction and provide the mechanical properties required for the intended application.

Tortuosity is another factor that has an impact on mass transport, affecting the nutrients' effective diffusivity and the cell migration rate within the scaffold [69]. The tortuosity refers to the path that the culture medium has to take through the interconnected pores to get from one extremity of the scaffold to another. Thus, scaffolds with high tortuosity present high resistance to fluid passage through the porous structure, resulting in low permeability.

Pore size should also be appropriate to allow for cell spreading and network formation and its optimal value usually depends on the material of the scaffold and the cell type [25]. According to Fu and Wang [74], the optimal mean pore diameter is the approximate diameter of the cell. This is because pore size establishes the proximity between the cells in the initial stages of the culture and the space available for their 3D organization during tissue development [69]. Although large pores can enhance cell proliferation, excessively large pores can be prejudicial to the mechanical properties of the structure [75] and discourage the extracellular matrix synthesis between the fibers [76].

In fibrous scaffolds, mean fiber diameter can affect the scaffold hydrophilicity, mechanical strength, porosity, pore size mean values, and distribution. In PLGA [77] and PCL [78] electrospun scaffolds, smaller fiber diameters were associated with more hydrophobic structures. However, even though scaffolds with larger fibers presented improved cell attachment due to higher hydrophilicity, the decreased available surface area led to reduced stem cell growth rates [78]. Microfibrous PLGA/PCL scaffolds with different fiber diameters presented similar ultimate tensile strength, but thicker fibers resulted in stiffer and less ductile scaffolds, associated with higher cell infiltration (due to pore size) and poor ECM production [79]. In a range from 1 to 2.5 μm, electrospun scaffolds with higher fiber diameters can be associated with higher porosity [80]. However, in a range of 1 to 10 μm, fiber thickness may not present a linear correlation with the porosity [81–83]. Elsayed et al. [80] observed the highest levels of cell infiltration and migration through the electrospun scaffolds with the largest pore size and greatest porosity. In addition, scaffolds with smaller fiber diameters present smaller pores [82, 84], which can hinder cell migration and colonization [58]. Furthermore, while electrospun scaffolds with smaller fiber diameters can present higher human MSC densities at the beginning of the in vitro cell culture, larger fiber diameter scaffolds can influence the cellular phenotype and differentiation [85].

Figure 3 presents a scheme for a porous structure where the architectural features discussed above are illustrated.

# 4 Culture conditions

The culture conditions directly affect cell behavior and tissue development in vitro. Parameters such as pH, osmolality, and temperature should be kept in an optimal operating range to ensure the viability of the cells. Other factors, like nutrient and metabolite concentrations, can be used to induce a specific cell reaction. Thus, some key culture variables that influence the cell culture are discussed below.

## 4.1 pH and osmolality

The main reason for pH variation in the culture medium is the production of carbon dioxide by metabolic processes. The most appropriate pH for the majority of mammalian cells is between 7.2 and 7.4 [86]. The decrease of the pH of the culture medium leads to lower cell proliferation and glucose uptake rate [87]. Alkaline microenvironments do not affect human bone marrow-derived MSC proliferation, but may inhibit ECM production and affect the differentiation potential of the cells [88]. A buffer of bicarbonate-carbon dioxide provides an excellent control of the pH while the cell culture remains in an incubator (usually with 5% $CO_2$) [89].

Cells need an isotonic environment because of the necessity to maintain the osmotic pressure over the culture, usually between 260 and 320 mOsm/kg [90]. Hypo and hyperosmotic cultures, when compared to cultures with a physiologic osmolality, can present smaller extracellular matrix (ECM) synthesis and reduced cell metabolism, and in extreme cases lead to cell death [91]. Hypertonic stress results in vesicle formation, increased cell area, and reduced
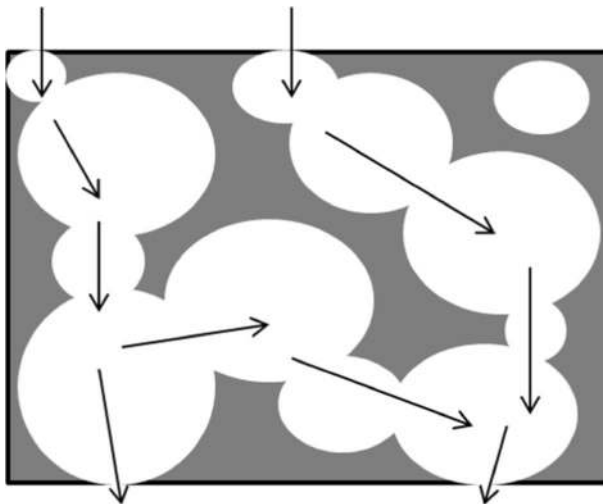


**Fig. 3** Architectural features of three-dimensional scaffolds. The porosity (void fraction) is indicated by the amount of *blank space* and the pore size and geometry is represented by the *size and geometry of the blank spaces*; the tortuosity is illustrated by the paths signaled by *black arrows*

proliferation in monolayer cultures of adipose-derived stem cells, with reduced cell viability in three-dimensional cultures [92].

## 4.2 Oxygen concentration

Oxygen levels lower than the atmospheric concentration (21%, v/v) can characterize a hypoxia condition and are part of the physiologic conditions found in vivo in the microenvironment of several stem-cell types (1–8%, v/v) [93]. Under hypoxia, oxygen is not only a nutrient but becomes a signaling molecule that acts on cell development and organization [94]. Human MSCs under hypoxia initiate the exponential phase of growth earlier and have reduced nutrient uptake and inhibitory metabolite production, when compared to cell cultures in normoxia [95].

The culture of human MSCs under hypoxia can modify the conversion of glucose in lactate (gradual accumulation of lactate) and change the energy production metabolism from aerobic to anaerobic [96]. Cell expansion under this condition can also affect the differentiation potential of MSCs through the up-regulation of the transcriptional expression of HIF-2$\alpha$ [97]. Low oxygen tensions can be used in rotating bioreactors but can lead to reduced and non-uniform ECM component deposition and, consequently, smaller tissue size [98].

## 4.3 Glucose concentration

Glucose is an important metabolic fuel and a limiting nutrient for MSC culture because their ATP production occurs mainly through glycolysis, which leads to the degradation of glucose into pyruvate [99]. According to Machado [100], glucose concentrations of approximately 5 mM propitiate higher viability and proliferation of human dental stem cells. Glucose can also affect the oxygen uptake rate of chondrocytes, resulting in near anoxia region formation in scaffolds cultivated with low glucose medium [101]. Furthermore, cell viability has shown to be hindered by carbon sources and not oxygen availability in 3D tumors [102].

Glucose concentration can drop drastically to 0.5 or 1.5 mM, within 3 days in cell cultures with low glucose medium, under hypoxia and normoxia, respectively, leading to reduced cell viability [103]. According to Deschepper et al. [96], combined low oxygen and glucose depletion leads to cell shrinkage and decreased cell viability and ATP production. Furthermore, not a single viable cell is observed after 3 days in cultures with no glucose with or without bovine fetal serum addition (which contains a small glucose concentration).

On the other hand, high glucose conditions can suppress bone-marrow MSC proliferation and migration [104]. This condition can activate glycogen synthase kinase-3$\beta$ (GSK3$\beta$), which inhibits the expression of cyclin D through the Wnt/$\beta$-catenin pathway, reducing cell proliferation. Simultaneously, the migration ability of the cells is reduced by the activation of GSK3$\beta$, which can decrease C-X-C chemokine receptor type 4 (CXCR4) expression via stromal cell-derived factor 1 (SDF-1)/CXCR4 signaling [104].

## 4.4 Toxic metabolite concentration

In glycolysis, cells convert pyruvate by lactate dehydrogenase (LDH) to lactate and this can lead to lactate accumulation at high glycolytic rates due to the increase of lactate production and efflux from the cells [105]. Mammalian cells, including MSCs, can also produce energy through glutaminolysis, generating ammonia and glutamate by hydrolysis of glutamine and lactate or alanine by further conversion of pyruvate [106]. The accumulation of toxic

metabolites such as lactate and ammonia can change the pH and the osmolality of the culture medium and inhibit cell growth. Lactate concentrations up to 20 mM inhibit MSC growth from the fifth day of cultivation [107]. According to Schop et al. [106], the source of the MSCs can influence cell metabolism and the capacity of the cells to tolerate high concentrations of toxic metabolites.

Metabolite concentration can also affect cell morphology, changing the fibroblast form of the MSCs to a more stretchy or cubic morphology. This can be related to the alkalinization or acidification of the cytoplasm, induced by high lactate and ammonia concentrations, respectively. However, human MSCs do not lose their differentiation potential when their growth is hindered by high amounts of lactate or ammonia in the culture medium [106].

## 5 Bioreactors

Dynamic culture systems, such as spinner flasks, rotating systems, and perfusion bioreactors (Fig. 4), can be used to reduce mass transport limitations in vitro and/or to optimize a specific process, such as cell expansion, differentiation, extracellular matrix (ECM) synthesis, or growth factor secretion. A dynamic culture more efficiently mimics the natural environment in which the scaffold will be transplanted afterwards because it can regulate the cell microenvironment and simulate different conditions of oxygen and shear stress [108]. Furthermore, bioreactors can be designed to control time and spatial cell signaling through the incorporation of biological or physical stimuli [109].

Spinner flask and stirred tank bioreactors (Fig. 4a) have been widely used to expand MSCs in commercial microspheres, which are also called microcarriers, due to the enhanced mass transport inside the constructs and resultant higher cell growth [110]. In order to optimize MSC growth, different microcarriers [111], culture medium [111–113], and shear stress levels [114] have been studied in stirred bioreactors. However, contrary to microcarriers, tissue substitutes require appropriate geometry and functions, usually being cultivated in dynamic systems with perfusion and rotation (Fig. 4b-f). Regarding engineered 3D scaffolds, the use of bioreactors in tissue engineering constitutes an alternative for providing appropriate nutrient supply, residual removal, gas exchange, and mechanical forces stimulus for cells [68].

Rotating wall bioreactors (Fig. 4b) provide mechanical stress stimulation, which induces osteogenic and chondrogenic differentiation [115]. This system involves lower shear stress



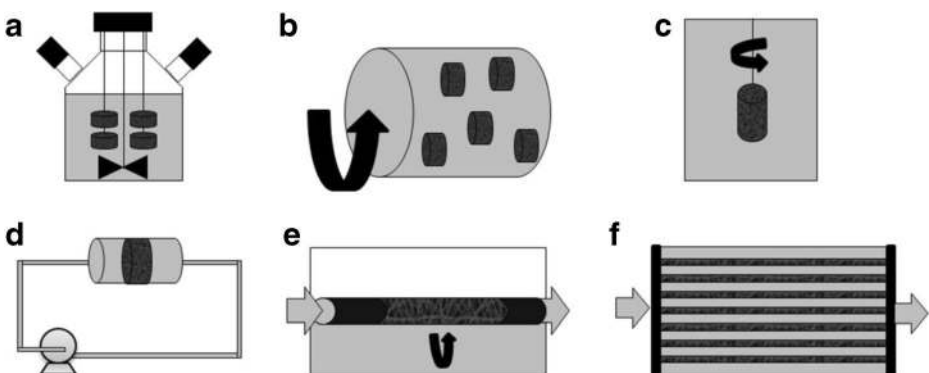Fig. 4 Bioreactor types for cell culture in tissue engineering (culture medium in *gray*, air in *white*): spinner flask (**a**), rotating wall (**b**), rotating bed (**c**), perfusion (**d**), rotating bed perfusion (**e**), and hollow fiber (**f**)

than other dynamic culture systems, while also resulting in homogeneous cell distribution due to enhanced mass transport. In a similar way, bioreactors with a rotating bed (Fig. 4c), where the scaffold rotates instead of the bioreactor wall, have been used to cultivate human umbilical vein smooth muscle cells in tubular electrospun scaffolds. Elsayed et al. [80] showed that a rotation dynamic system promoted cell infiltration through the scaffold thickness and increased cell proliferation when compared to a static culture.

Other bioreactors use flow perfusion (Fig. 4d) to provide higher nutrient transport, leading to enhanced cell viability and uniform distribution through 3D scaffolds [116]. Higher cell growth, osteoblastic differentiation induced by the shear stress [71, 117–119], and cell migration [120–123] are often observed in perfusion bioreactors when compared to static culture. Furthermore, oxygen concentration gradients can be produced in perfusion bioreactors to mimic in vivo ECM conditions and enhance cell migration and growth [124].

Direct perfusion bioreactors have also been shown to enhance ECM deposition and distribution [119, 125]. Liao et al. [126] used perfusion bioreactors to generate an ECM coated in electrospun microfibrous scaffolds by cultivating chondrocytes and then decellularizing the construct. The constructs were later used for MSC chondrogenic differentiation under serum-free conditions and with no transforming growth factor beta 1 (TGF-β1) addition. Thibault et al. [127] also used perfusion flow to induce ECM deposition by MSCs in an electrospun scaffold followed by decellularization of the construct and reseeding with MSCs, but used osteogenic medium and focused on osteogenic differentiation.

In direct perfusion systems, it is important to establish an optimal perfusion flow rate to avoid cell death due to high shear stress [118]. Small pores can also result in high shear stress levels, with bioreactor cultures being performed mainly with porous matrixes with mean pore sizes in the range of 100 to 500 μm, which are not possible in electrospun scaffolds (maximum mean pores of 45 μm reported by Pham et al. [82]). The perfusion culture of human MSCs seeded in electrospun nanofibers can lead to initial round-shaped morphology and may result in cell proliferation, chondrogenic differentiation, and ECM synthesis, similarly to what is observed in static culture [128]. Gugerell et al. [129] also obtained no improvement with direct perfusion of MSCs seeded in hydrogels or on top of the bottom layer in stacked electrospun scaffolds.

One alternative to reduce shear stress inside the pores in perfusion systems is to use a bypass to release pressure build-up [130]. Fixed-bed fibrous bioreactors can also allow for lower shear stress inside electrospun scaffolds [131]. Yeatts et al. [132] used an indirect perfusion system with flow through a packed bed of electrospun scaffolds seeded with human MSCs to produce tissue substitutes for further subsequent implantation into rat femoral condyle defects. Kim and Ma [133] compared two indirect perfusion systems with parallel flow and transverse flow for growth factor secretion by human MSCs in 3D constructs. It was verified that parallel flow allowed for cell-secreted basic fibroblast growth factor (FGF-2) accumulation in the scaffolds whereas transverse flow increased the mass transport through the scaffold and affected FGF-2 redistribution in the construct.

For direct perfusion, da Silva et al. [128], Grayson et al. [134], Dahlin et al. [135], and Santoro et al. [136] used a system in which the flow split in several channels, reaching lower flow rates and reducing shear stress in electrospun scaffolds. However, the culture medium was the same for all the scaffolds and it was not possible to control the individual metabolite production, nutrient consumption, and flow because each scaffold has a random geometry and consequently results in a different resistance to flow, as highlighted by Dahlin et al. [135].

On the other hand, medium perfusion and scaffold rotation can be combined in a direct perfusion bioreactor with rotating bed (Fig. 4e). Diederichs et al. [137] compared the culture of human MSCs seeded in macroporous ceramic scaffolds in static conditions and in a direct perfusion bioreactor with rotating bed. Under the proposed dynamic conditions, high glucose consumption and lactate production indicated increased cell proliferation. In addition, the bioreactor promoted enhanced osteogenic differentiation. Neumann et al. [138] also expanded human MSCs in a perfused rotating bed (cell carrier slides), but used a disposable bioreactor. Their dynamic culture scheme provided low shear stress and high cell yields while maintaining MSC morphology and stemness characteristics (specific MSC surface markers and osteo/ adipo/chondro lineages differentiation potential).

Tubular electrospun scaffolds have also been seeded with human MSCs for cultivation in rotating bed perfusion bioreactors with alternate exposure to air and culture medium phases. This dynamic culture system, when combined with appropriate growth factors and serum amounts, stimulated MSC differentiation into a smooth muscle cell phenotype [139]. The bioreactor culture also increased ECM synthesis and deposition and the homogeneity of cell distribution on the scaffold surface; it also presented cell colonization inside the scaffold, which was not observed in static culture due to small pore size [139].

Another dynamic system that has been used to produce bone tissue substitutes with MSCs is the hollow fiber bioreactor (Fig. 4f), in which cells are seeded in the extracapillary space and culture medium flows inside the hollow fiber lumen [140]. Furthermore, higher cell density, proliferation, and osteogenic differentiation can be achieved by 3D scaffolds seeded with MSC cultures in bioreactors with combined perfusion and cyclic compression [141]. Furthermore, in order to generate functional tissue responsive to both mechanical and electrical signaling, MSCs have been incorporated in electrospun fibers and cultivated in bioreactors with dynamic uniaxial strain and electrical stimulus [21].

# 6 Cell seeding

The seeding density of cells can influence tissue development because high cellularity increases the cell–cell contact and communication. However, its effect is not so evident when cells become confluent with culture time, which occurs with high cell concentrations in long-term cultures [142]. Cell seeding methods can be static (droplet or suspension) or dynamic (agitation, vacuum, centrifugation, stirring, rotational, and perfusion), observing that in some cases (stirred, rotational, and perfusion) bioreactors can be used for cell seeding by using a cell suspension instead of the culture medium [143]. As the seeding methods affect the quantity and the distribution of viable cells adhered to the scaffolds at the beginning of the culture, the main features of these seeding methods, schematized in Fig. 5 (except for stirring, rotational, and perfusion, already presented in Fig. 4), are discussed below.

Static methods by droplet (Fig. 5a) or suspension (Fig. 5b) are simpler but have a low level of efficiency and superficial adhesion. Droplet seeding, for instance, can lead to 20–50% of cells not being attached to the scaffold due to breakup of the cell suspension and further floating of the cells [76]. Yamanaka et al. [144] used an alternative droplet seeding in which the floating of MSCs was avoided by using an absorbent surface under the scaffold to force the flow of cell suspension from the top to the bottom of the scaffold. However, there is no evidence that this would be an effective solution for electrospun scaffolds, as they used scaffolds produced by solvent casting and particulate leaching, with large and interconnected pores.
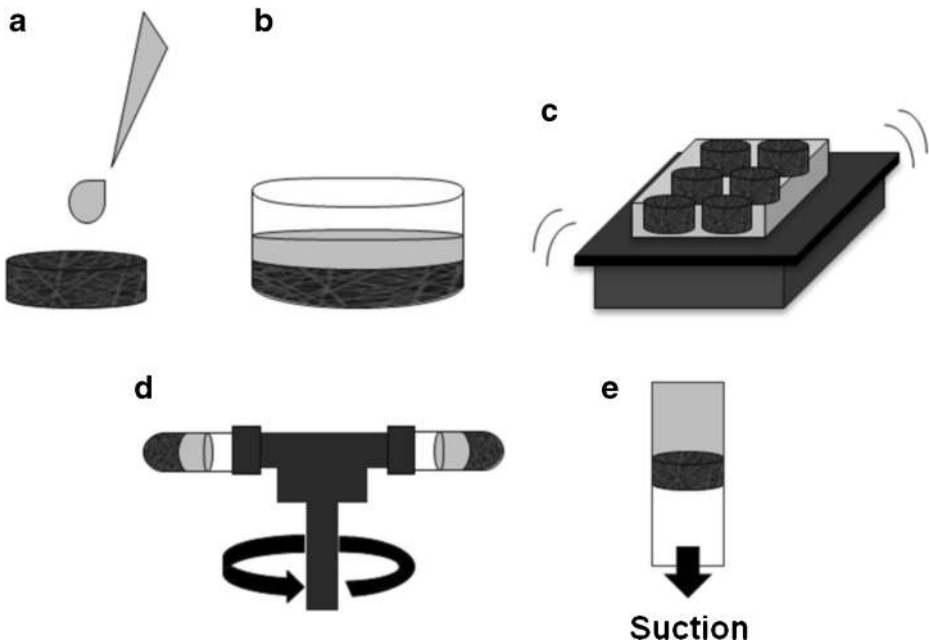
**Fig. 5** Seeding methods (cell suspension in *gray*): droplet (**a**), suspension (**b**), agitation (**c**), centrifugation (**d**), and vacuum (**e**)

Other methods, such as vacuum seeding (Fig. 5e) [145] and centrifugation seeding (Fig. 5d) [146, 147] require small cell quantities and can be applied to reduce the time of the procedure, increase cell infiltration, and homogenize their distribution in 3D scaffolds. However, scaffold porosity and pore size may affect the results of both vacuum [148] and centrifugation [147] seeding. Accordingly, different systems and protocols result in distinct seeding efficiencies and even optimized protocols for these methods can lead to results inferior to those with static seeding [144]. Furthermore, Griffon et al. [143] studied MSC attachment with several seeding techniques and verified that the scaffold material and structure could be determinant in seeding efficiency.

Regarding electrospun scaffolds, Wanasekara et al. [149] observed that nanofiber and microfiber structures presented different fibroblast infiltration and may require distinct vacuum pressures to optimize cell distribution inside the scaffolds. In addition, epithelial cells have presented higher viability with the centrifugal method than with static seeding [150].

The most widely used dynamic methods are stirring (Fig. 4a), agitation (Fig. 5c), and perfusion (Fig. 4d) seeding. The first two have higher efficiency levels than static methods, but the amount of adhered cells depends on the cell concentration in the seeding solution [151]. Perfusion systems have higher efficiency levels and lower standard deviations for the number of cells adhered to scaffolds than static seeding methods [76]. When compared to droplet or stirred seeding, perfusion presents higher cell viability and uniformity of cell distribution [152]. A rotating bed scheme (Fig. 4e) can be used in perfusion bioreactors to increase the homogeneity of the cell distribution inside 3D scaffolds [125]. Besides this, perfusion seeding can be optimized, considering the inverse correlation between flow rate and cell seeding efficiency. Due to these characteristics, perfusion bioreactors have been used for seeding in a variety of systems, including ceramic scaffolds with goat MSCs [125], fibrous scaffolds with

human MSCs [153], electrospun scaffolds with human fibroblasts [76], and rat MSCs [154] for subsequent cultivation.

The thickness of electrospun scaffolds is limited by the reduction of fiber deposition efficiency caused by the insulating effect of deposited fibers and consequent reduction of electrostatic force applied to the polymeric solution [155]. For applications that require a high volume of tissue, thin scaffolds can be assembled in a multilayer form to obtain the desired thickness [156–160]. According to Ardakani et al. [161], cells cannot detach from one layer and adhere to an adjacent layer naturally, especially when there is liquid between the surfaces. Thus, in multilayered configurations, the position and disposition of the seeding surfaces can be important for the final cell distribution and the drag of cells with the passage of the flow.

## 7 Modeling scaffold properties and impacts

Modeling methods are mainly used to determine 3D scaffold architectural properties or analyze their impact on nutrient transport and cell growth, adhesion, deformation, and detachment [162–170]. In addition, the process of scaffold degradation can also be studied and modeled to evaluate tissue development [171–176].

Truscello et al. [169] used a computational fluid-dynamic (CFD) model to predict 3D scaffold permeability with different pore sizes and resulting different porosities. Santamaría et al. [168] also used a CFD model to determine permeability and wall shear stress under diverse flow rates for heterogeneous 3D structures with different pore sizes and interconnectivity. Mechanical and biological properties of electrospun nanofibrous scaffolds can also be estimated with mathematical models. Gómez-Pachón et al. [164] predicted the effective Young's modulus of scaffolds with aligned or random fiber disposition, while Decuzzi and Ferrari [163] estimated the cellular adhesion strength as a function of the scaffold roughness and surface energy. These models can be helpful in the design of scaffolds and bioreactors and in situations where experimental measurements of these parameters are not available.

Coletti et al. [162] evaluated the effect of scaffold porosity and permeability variation due to cell density on cell growth and mass transport in 3D perfusion cultures. Simulation results showed that nutrient availability and cell density decrease with time in deeper sections of the scaffold as a result of the pore volume occupation by cells as they proliferate and the consequent reduction of the scaffold porosity and permeability. This could indicate that initial cell density and distribution must be optimized in accordance with the scaffold pore size in order to generate homogeneous tissue. Figure 6 shows different pore obstruction and size reduction as a result of cell adhesion and growth.

Jungreuthmayer et al. [165] used CFD modeling to study cell drag and shear stress through scaffolds with different pore sizes under flow perfusion. It was observed that cells with bridged morphology (adhered to more than one strut) were up to 500 times more deformed when subjected to the same shear stress than cells with a flat morphology (adhered to only one strut). Thus, cell morphology, when adhered on the scaffold pore, could determine its detachment under perfusion. McCoy and O'Brien [167] studied the influence of scaffold pore size in cell attachment and detachment under different perfusion flow rates, and correlated cell deformation with cell detachment through experimental and computational techniques. The proposed model could predict cell loss under different flow perfusion as a function of the initial cell number, mean pore size, and mean shear stress, and included a constant for cell growth in static
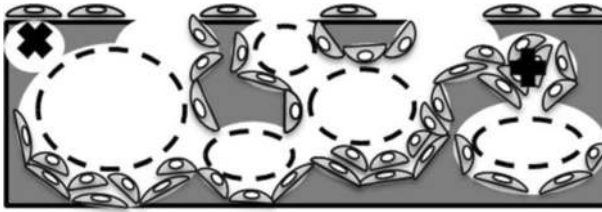
**Fig. 6** Pore obstruction with cell growth: *dashed circles* represent the reduction of the pore size with cell adhesion on the pore walls; the "*x*" symbol denotes the obstruction of superficial small pores with cell adhesion on the scaffold surface and the "+" symbol indicates pore obstruction due to cell growth and full occupation of the pore space

cultures. Thus, their model could be used to determine the conditions that minimize the effect of pore obstruction with cell proliferation.

Ma et al. [166] evaluated the effect of porosity in perfusion flow through scaffolds and observed that smaller porosities and pore sizes presented higher velocities due to the restriction of available space for fluid flow and consequent increase of pressure drop. In addition, low-porosity scaffolds presented higher oxygen volume fraction, indicating reduced consumption and thus smaller cell growth. Yan et al. [170] studied the effect of different initial porosities and flow rates on glucose and oxygen transport and on cell growth within 3D scaffolds, taking into consideration the increase of the scaffold porosity due to polymer degradation. It was observed that high initial porosities can reduce nutrient-effective diffusivity and availability with time due to the occupation of the void space by cells and, as a result, affect cell distribution inside the scaffold. This model could be useful for scaffolds with rapid degradation times and corroborates with the results of Coletti et al. [162] and McCoy and O'Brien [167].

Scaffold degradation has also been studied using complex models. Chen et al. [172] developed a mathematical model of the hydrolysis reaction and autocatalysis and considered the effect of mass transport to evaluate the polymeric degradation of microparticles and tissue scaffolds. The stochastic hydrolysis process was described based on a pseudo first-order kinetic equation. The probability of hydrolysis of a single element was modeled as a probability density function dependent on the structural porosity and on the average molecular weight loss. The autocatalytic contribution was modeled as an exponential function of the acid catalyst. The model was able to predict the experimental behavior of degradation and erosion of bulk-erosive polymer structures and evaluated the impact of scaffold architecture and mass transfer on the degradation of porous structures.

Heljak et al. [174] modeled the aliphatic polyester hydrolytic degradation of a 3D porous scaffold using reaction-diffusion equations for the concentrations of ester bounds and monomers, and also considered the autocatalytic effect of soluble monomers. The model could predict the degradation time and changes in the molecular weight and mass of a bone scaffold. At a later date, these authors used this model to study the effect of different porosities on the degradation process of a poly(DL-lactide-*co*-glycolide) scaffold under dynamic or static conditions. Simulation results indicated that high porosity, fluid flow, or periodic replacement of the medium (in static conditions) could reduce polymeric scaffold degradation [175]. The model could be used to optimize scaffold porosity and to determine when medium replacement is necessary in static culture, based on the accumulation of degradation by-products.

Shazly et al. [176] developed a computational model of bulk hydrolysis of bioresorbable vascular poly(L-lactide) scaffolds in a post-implantation in vivo environment. The authors studied the degradation by-product transport via diffusion and convection by considering the

blood flow (in the lumen and the porous arterial wall) when the erodible scaffold is implanted within the arterial wall. The polymer degradation and autocatalysis was modeled as a first-order reaction with a system of reaction-diffusion equations that considered the systematic formation of four oligomer groups and lactic acid. The metabolism of lactic acid in a healing zone with varying diffusivity (to account for tissue remodeling) and in the arterial wall was described as a first-order reaction and incorporated in reaction-diffusion-convection equations. The model could predict the levels of lactic acid that accumulate in local tissue by coupling its production with convective and diffusive transport and metabolic elimination. It was observed that the interplay between the tissue remodeling and the hydrolysis process regulates the levels of degradation by-products within the tissue and that mass transport is a more effective by-product clearance mechanism than metabolic elimination. This model was later used to evaluate the effect of polydispersity, initial degree of crystallinity, and lactide doping in the degradation, erosion, and by-product accumulation. It was observed that only the erosion process was sensitive to crystallinity and that all processes were responsive to lactide doping [173].

Akalp et al. [171] proposed a model of tissue growth, enzymatic degradation of an enzyme-sensitive hydrogel, and ECM molecules transport within the hydrogel scaffold. Enzymes released by the cells were considered to diffuse through the polymer network and degrade the hydrogel through cross-link cleavage, following Michaelis–Menten kinetics. The transport and deposition of ECM molecules secreted by the cells were modeled with a convection-diffusion-reaction system, considering an inhibition term for ECM deposition. It was shown that an appropriate relationship between scaffold degradation and ECM transport and deposition is necessary to maintain the mechanical properties of the structure. The discussed degradation models could be used in scaffold design to optimize the relationship between architectural and degradation properties.

## 8 Modeling for bioreactors, seeding methods, and culture conditions analysis

Modeling can also be used as a tool for bioreactor design [177–181], seeding process analysis [157, 182–184], and culture condition analysis and optimization [22, 134, 162, 185–193].

Singh et al. [181] used CFD modeling to study the velocities and wall shear stress inside and outside a scaffold under uni-axial and bi-axial flow schemes in a rotational bioreactor. It was observed that bi-axial rotations were capable of increasing fluid velocities and shear stress within the scaffolds by combining rotational velocity vectors. This model could be useful in rotational bioreactor design and optimization in a simplified study as nutrient transport and cell growth are not considered.

Pathi et al. [179] studied parallel perfusion bioreactors with different liquid layer thicknesses above a porous scaffold seeded with granulocyte progenitor cells. Oxygen supply was increased with a larger liquid layer thickness due to the higher oxygen delivery through hydrodynamic flow, with little contribution of the oxygen permeability of the outer membrane. Through computational modeling, it was possible to verify that convective oxygen delivery provided by culture medium perfusion could overcome diffusion limitations and enhance cell growth.

Devarapalli et al. [177] used CFD modeling to simulate several perfusion bioreactor designs with rectangular or circular shapes and different inlet and outlet flow configurations in order to evaluate the resulting shear stress and pressure drop in porous scaffolds.

Homogenous shear stress distribution could be achieved in circular bioreactors with semicircular inlet and outlets. Hidalgo-Bastida et al. [178] also performed CFD simulations to compare circular and rectangular shape perfusion bioreactors, but did not evaluate diverse inlet and outlet shapes. On the other hand, a proposal was made for a mixed design with a rectangular holder for circular scaffolds and a safe distance between the scaffold and the inlet and output to guarantee uniform flow and shear stress through the scaffold.

Schirmaier et al. [180] used mathematical models to determine optimum values for impeller speeds and local shear stress in stirred single-use bioreactors for human adipose tissue-derived MSC expansion under low-serum conditions. With the help of simulation results, it was possible to scale-up microcarrier-based cell cultures from spinner flasks to large-scale stirred single-use bioreactors. Thus, CFD modeling could be used not only in the design step but also in the scale-up of bioreactors to guarantee the required conditions for cell expansion and tissue development.

The generation of homogeneous tissue can also be affected by the seeding process with an initial homogeneous cell distribution not necessarily being the best alternative in tissue engineering. Doagă et al. [194] proposed a non-linear kinetic model of cell adhesion in porous scaffolds based on the Langmuir's theory of adsorption to describe cell seeding in a stirred bioreactor. Cell attachment was considered a two-step process with initial recovery of the cell integrin function—inhibited after the trypsinization required for cell detachment from the culture flask for cell counting before cell seeding—and further integrin binding with scaffold sites available for cell attachment. The model was able to represent the experimental process of cell adhesion and reinforced the higher cell seeding efficiencies obtained in protocols with alternative cell detachment treatments other than trypsinization.

Dunn et al. [157] proposed an alternating cell-seeding strategy for multilayer matrices to surpass oxygen depletion in the inner core of the scaffold, verified with computational simulations. Modeling cell growth and nutrient transport in a homogeneously seeded scaffold showed the formation of hypoxic regions with time as the cell consumption became higher than oxygen delivery through diffusion. Chung et al. [182] compared the result of various seeding modes in cell growth in scaffolds and proposed that cell seeding in only the middle portion of the scaffold could increase nutrient availability and homogenize cell distribution and growth in tissue-engineered constructs.

In addition, Jeong et al. [184] evaluated the effect of different seeding strategies on cell growth, and identified an optimal set of parameters for obtaining a homogeneous cell distribution in five stacked scaffolds through mathematical modeling. It was observed that the interplay between cell growth and nutrient consumption could be optimized by alternating seeding between unseeded and partially cell-seeded scaffolds (with cells seeded in concentric annulus) (Fig. 7). These models could be used to develop new strategies for optimal cell seeding based on specific cell proliferation, migration, and nutrient consumption.

Several modeling applications aim to evaluate and/or identify optimal culture conditions (flow rate, shear stress, fluid velocity, oxygen tension, electrical potential) within scaffolds cultivated in bioreactors. Raimondi et al. [192] used CFD modeling to predict shear stress and fluid velocity in 3D fibrous structures under perfusion. Grayson et al. [134] optimized medium perfusion rate for a direct perfusion bioreactor by predicting the shear stress inside the scaffold. Through mathematical modeling, it was possible to evaluate the oxygen transport and verify if the oxygen levels and cell viability were maintained in a range of flow rate values. These models could be used to characterize the bioreactor conditions that cannot always be experimentally measured, such as shear stress and oxygen concentration.
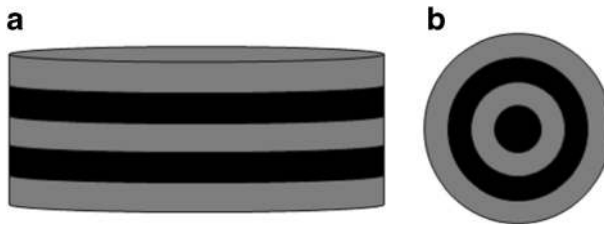
**Fig. 7** Different cell-seeding strategies proposed by Jeong et al. [184]: seeded scaffold (*gray*) intercalated with non-seeded scaffolds (*black*) (**a**) and scaffolds seeded in alternating concentric annulus regions (**b**)

Flaibani et al. [188] used mathematical modeling to identify an optimum flow rate for reaching a maximum cell volume fraction inside 3D scaffolds under perfusion. To achieve this, cell growth was modeled as a function of pore size distribution and oxygen concentration. It was observed that low flow rates could inhibit cell growth by leading to very low oxygen concentrations (hypoxia) inside pores with different diameters. On the other hand, high flow rates resulted in elevated shear stress levels that could inhibit cell growth or induce cell detachment. This model could be used to estimate cell growth and distribution inside heterogeneous porous scaffolds.

Another option to account for scaffold microorganization was reported by Porter et al. [191]. The authors used microcomputed tomography imaging to define scaffold microarchitecture. Local shear stress was then estimated at various perfusion flow rates to determine an optimal value through association with experimental data of cell growth in the literature. A peak in shear stress of 57 mPa was observed and associated with cell death within the constructs. This model could be used to define limiting and optimal values of local shear stress for cell growth as a function of scaffold microarchitecture.

Chung et al. [187] predicted shear stress levels inside a scaffold under direct perfusion as a function of pore size and its reduction with cell growth. It was observed that the macro average stress could have a fivefold increase and that the overall permeability could be reduced dramatically with a slight overall cell volume fraction increase. These changes were associated with the reduction of the scaffold void space with pore occupation by cell and ECM volumes. In the same context, Lesman et al. [189] developed a CFD model to predict the shear stress and pressure drop with different flow rates in 3D cultures under direct perfusion. A cell-layer thickness was considered to account for cell-growth impact on the pore space reduction and on the scaffold mass transport. The simulations show that shear stress average values increased with time due to cell growth and thickening of the cell layer inside the pores, which corroborates with the time decrease of scaffold permeability constant obtained experimentally. These models could be used to predict permeability and shear stress values for scaffolds with high density of cells or small pore sizes.

Sacco et al. [195] proposed a model where the cells and the ECM compose a biomass phase and the maximum biomass growth rate of the Monod kinetics is a function of shear stress. However, nutrient concentration and shear stress variation in time and space were not considered. Liu et al. [190] compared static and dynamic cultures under direct perfusion with different flow rates using a CFD model that considers both nutrient availability and shear stress stimulation on cell-growth kinetics. The cells and the ECM components secreted by the cells were also considered as one single phase in a way whereby it is possible to use these models to consider the shear stress effect on cell growth by stimulation of the ECM synthesis under perfusion.

Zhao et al. [193] used a mathematical model to predict shear stress and oxygen levels inside 3D poly (ethylene terephthalate) (PET) scaffolds under perfusion; three matrices were assembled in series in each perfusion chamber. The simulation results indicated that different flow rates did not yield changes in oxygen levels that could affect cell growth and metabolism. Furthermore, while increased human MSC growth and ECM deposition were observed at low flow perfusion, higher flow rates could upregulate the osteogenic differentiation potential of the cells. Thus, this model was helpful to indicate that shear stress levels could be an important factor regulating human MSC development in 3D scaffolds.

Coletti et al. [162] simulated two flow conditions in a perfusion bioreactor—partial flow (flow channelized through a gap between the scaffold and the bioreactor wall) and total flow perfusion through the scaffold. They studied their impact on oxygen transport and cell growth. The channeling of flow perfusion can occur experimentally as a result of the lack (when this bypass is required and designed to reduce shear stress levels inside the scaffold) or insufficiency of the sealing system. Simulation results were compared and showed that partial perfusion could affect oxygen delivery by reducing convection inside the scaffold and, as a consequence, could reduce the construct cell density. Thus, this model could be used to evaluate operational flaws and also to design bioreactor bypasses in order to optimize flow conditions and cell growth inside 3D scaffolds.

One example of a partial perfusion bioreactor is given by Campolo et al. [185], where a gap around the scaffold is designed to serve as a by-pass flow. The authors proposed a modeling approach to determine an appropriate flow rate to obtain homogeneous cell distribution in 3D scaffolds under indirect perfusion. Mass transport and reaction information was used in association with flow regime characteristics to calculate the required perfusion flow to maintain a target cell growth rate.

In addition to flow perfusion, electrical variables have also been modeled in bioreactors for tissue engineering purposes. Maidhof et al. [22] characterized the electrical potential of a perfusion bioreactor by modeling its generation and evaluating the electrical field where cardiac constructs were placed. It was observed that the electric potential drop was quite linear and constant through the scaffold length. This model was helpful in validating the generation of scaffolds as functional cardiac constructs exposed to the same electrical field.

# 9 Conclusions

The main tissue-engineering challenges are related to scaffold design, mass transport, and cell infiltration and colonization within the scaffolds. In addition, culture conditions affect cell behavior and vary from one study to another, making the comparison of different experiments difficult. In order to control and study these conditions, bioreactors and modeling techniques can be applied. Regarding the dynamic culture of mesenchymal stem cells in electrospun scaffolds, the cell proliferation and differentiation, and the secretion of growth factors and extracellular matrix components have been studied in different systems and under several culture conditions. Bioreactors with electrical and mechanical stimulation have also recently been studied for the development of functional tissue responsive to these stimuli. However, tissue vascularization, which is important for the maintenance of cell viability in vivo after transplantation, is not always evaluated in bioreactor studies. In addition, the co-culture of stem cells and other cell types in bioreactors could reveal important features of tissue function as shear stress and other factors present in dynamic conditions could affect the development of

multicellular 3D cultures. While the bioreactor design has to be optimized according to the scaffold and cell characteristics, modeling has its own challenges. There are limitations in measurement techniques, which make it difficult to validate the model with respect to variables that cannot be measured directly. Thus, the combination of modeling and electrospun scaffolds for stem cell culture still requires research and improvement to fulfill its potential for optimizing tissue development.

**Compliance with ethical standards** This work does not contain any studies with human participants or animals performed by any of the authors.

**Conflict of interest** The authors declare that they have no conflict of interest.

# References

1. Langer, R., Vacanti, J.P.: Tissue engineering. Science **260**, 920–926 (1993). https://doi.org/10.1126/science.8493529
2. O'Brien, F.J.: Biomaterials & scaffolds for tissue engineering. Mater. Today **14**, 88–95 (2011). https://doi.org/10.1016/S1369-7021(11)70058-X
3. Chua, A.W.C., Khoo, Y.C., Tan, B.K., Tan, K.C., Foo, C.L., Chong, S.J.: Skin tissue engineering advances in severe burns: review and therapeutic applications. Burn. Trauma. **4**, 3 (2016). https://doi.org/10.1186/s41038-016-0027-y
4. Place, E.S., Evans, N.D., Stevens, M.M.: Complexity in biomaterials for tissue engineering. Nat. Mater. **8**, 457–470 (2009). https://doi.org/10.1038/nmat2441
5. Oryan, A., Alidadi, S., Moshiri, A., Maffulli, N.: Bone regenerative medicine: classic options , novel strategies , and future directions. J. Orthop. Surg. Res. **9**, 18 (2014). https://doi.org/10.1186/1749-799X-9-18
6. Fitzpatrick, L.E., McDevitt, T.C.: Cell-derived matrices for tissue engineering and regenerative medicine applications. Biomater. Sci. **3**, 12–24 (2015). https://doi.org/10.1039/C4BM00246F
7. Ku, D., Braddon, L., Wooton, D.: Poly(Vinyl Alcohol) Cryogel, (1999)
8. Kumar, R.J., Kimble, R.M., Boots, R., Pegg, S.P.: Treatment of partial-thickness burns: a prospective, randomized trial using transcyte (TM). ANZ J. Surg. **74**, 622–626 (2004). https://doi.org/10.1111/j.1445-1433.2004.03106.x
9. Walsh, W.R., Bertollo, N., Heuberer, P., Christou, C., Stanton, R., Poggie, R.: Evaluation of a PLLA device in-vitro and in an ovine model of acute rupture of the rotator cuff. In: Proceedings of the Orthopaedic Research Society Annual Meeting, Las Vegas, Nevada, 2015
10. Khojasteh, A., Behnia, H., Hosseini, F.S., Dehghan, M.M., Abbasnia, P., Abbas, F.M.: The effect of PCL-TCP scaffold loaded with mesenchymal stem cells on vertical bone augmentation in dog mandible: a preliminary report. J. Biomed. Mater. Res. Part B **101**, 848–854 (2013). https://doi.org/10.1002/jbm.b.32889
11. Flasza, M., Kemp, P., Shering, D., Qiao, J., Marshall, D., Bokta, A., Johnson, P.A.: Development and manufacture of an investigational human living dermal equivalent (ICX-SKN). Regen. Med. **2**, 903–918 (2007). https://doi.org/10.2217/17460751.2.6.903
12. Baskin, D.S., Ryan, P., Sonntag, V., Westmark, R., Widmayer, M.A.: A prospective, randomized, controlled cervical fusion study using recombinant human bone morphogenetic protein-2 with the CORNERSTONE-SR allograft ring and the ATLANTIS anterior cervical plate. Spine (Phila Pa 1976) **28**, 1219–1224; discussion 1225 (2003). https://doi.org/10.1097/01.BRS.0000065486.22141.CA
13. Kreuz, P.C., Müller, S., Ossendorf, C., Kaps, C., Erggelet, C.: Treatment of focal degenerative cartilage defects with polymer-based autologous chondrocyte grafts: four-year clinical results. Arthritis Res. Ther. **11**, R33 (2009). https://doi.org/10.1186/ar2638

14. Stone, P.A., AbuRahma, A.F., Mousa, A.Y., Phang, D., Hass, S.M., Modak, A., Dearing, D.: Prospective randomized trial of ACUSEAL versus Vascu-Guard patching in carotid endarterectomy. Ann. Vasc. Surg. **28**, 1530–1538 (2014). https://doi.org/10.1016/j.avsg.2014.02.017

15. Kehoe, S., Zhang, X.F., Boyd, D.: FDA approved guidance conduits and wraps for peripheral nerve injury: a review of materials and efficacy. Injury **43**, 553–572 (2012). https://doi.org/10.1016/j.injury.2010.12.030

16. Olson, J.L., Atala, A., Yoo, J.J.: Tissue engineering: current strategies and future directions. Chonnam Med. J. **47**, 1–13 (2011). https://doi.org/10.4068/cmj.2011.47.1.1

17. Chatterjea, A., Meijer, G., van Blitterswijk, C., de Boer, J.: Clinical application of human mesenchymal stromal cells for bone tissue engineering. Stem Cells Int. **2010**, 215625 (2010). https://doi.org/10.4061/2010/215625

18. Koh, C.J., Atala, A.: Tissue engineering, stem cells, and cloning: opportunities for regenerative medicine. J. Am. Soc. Nephrol. **15**, 1113–1125 (2004). https://doi.org/10.1097/01.ASN.0000119683.59068.F0

19. Tay, L.X., Ahmad, R.E., Dashtdar, H., Tay, K.W., Masjuddin, T., Ab-Rahim, S., Chong, P.P., Selvaratnam, L., Kamarul, T.: Treatment outcomes of alginate-embedded allogic mesenchymal stem cells versus autologous chondrocytes for the repair of focal articular cartilage defects in a rabbit model. Am. J. Sports Med. **40**, 83–90 (2012). https://doi.org/10.1177/0363546511420819

20. Wong, K.L., Lee, K.B.L., Tai, B.C., Law, P., Lee, E.H., Hui, J.H.P.: Injectable cultured bone marrow-derived mesenchymal stem cells in varus knees with cartilage defects undergoing high tibial osteotomy: a prospective, randomized controlled clinical trial with 2 years' follow-up. Arthrosc. - J. Arthrosc. Relat. Surg. **29**, 2020–2028 (2013). https://doi.org/10.1016/j.arthro.2013.09.074

21. Cook, C.A., Huri, P.Y., Ginn, B.P., Gilbert-Honick, J., Somers, S.M., Temple, J.P., Mao, H.Q., Grayson, W.L.: Characterization of a novel bioreactor system for 3D cellular mechanobiology studies. Biotechnol. Bioeng. **113**, 1825–1837 (2016). https://doi.org/10.1002/bit.25946

22. Maidhof, R., Tandon, N., Lee, E.J., Luo, J., Duan, Y., Yeager, K., Konofagou, E., Vunjak-Novakovic, G.: Biomimetic perfusion and electrical stimulation applied in concert improved the assembly of engineered cardiac tissue. J. Tissue Eng. Regen. Med. **6**, e12–e23 (2012). https://doi.org/10.1002/term.525.Biomimetic

23. Wang, Z., Teoh, S.H., Johana, N.B., Khoon Chong, M.S., Teo, E.Y., Hong, M., Yen Chan, J.K., San Thian, E.: Enhancing mesenchymal stem cell response using uniaxially stretched poly(ε-caprolactone) film micropatterns for vascular tissue engineering application. J. Mater. Chem. B **2**, 5898–5909 (2014). https://doi.org/10.1039/C4TB00522H

24. Knight, E., Przyborski, S.: Advances in 3D cell culture technologies enabling tissue-like structures to be created in vitro. J. Anat. **227**, 746–756 (2015). https://doi.org/10.1111/joa.12257

25. Lawrence, B.J.: Mass Transfer in Porous Tissue Engineering Scaffolds (PhD Thesis), Oklahoma State University (2008)

26. Romagnoli, C., Zonefrati, R., Galli, G., Puppi, D., Pirosa, A., Chiellini, F., Martelli, F.S., Tanini, A., Brandi, M.L.: In vitro behavior of human adipose tissue-derived stem cells on poly(ε-caprolactone) film for bone tissue engineering applications. Biomed. Res. Int. **2015**, 323571 (2015). https://doi.org/10.1155/2015/323571

27. Lawrence, B.J., Devarapalli, M., Madihally, S.: V: flow dynamics in bioreactors containing tissue engineering scaffolds. Biotechnol. Bioeng. **102**, 935–947 (2009). https://doi.org/10.1002/bit.22106

28. Asaoka, T., Ohtake, S., Furukawa, K.S., Tamura, A., Ushida, T.: Development of bioactive porous α-TCP/HAp beads for bone tissue engineering. J. Biomed. Mater. Res. Part A. **101**, 3295–3300 (2013). https://doi.org/10.1002/jbm.a.34517

29. Matsuno, T., Hashimoto, Y., Adachi, S., Omata, K., Yoshitaka, Y., Ozeki, Y., Umezu, Y., Tabata, Y., Nakamura, M., Satoh, T.: Preparation of injectable 3D-formed beta-tricalcium phosphate bead/alginate composite for bone tissue engineering. Dent. Mater. J. **27**, 827–834 (2008). https://doi.org/10.4012/dmj.27.827

30. Matsunaga, Y.T., Morimoto, Y., Takeuchi, S.: Molding cell beads for rapid construction of macroscopic 3D tissue architecture. Adv. Mater. **23**, 90–94 (2011). https://doi.org/10.1002/adma.201004375

31. Wang, J.: Porous Microbeads as Three-Dimensional Scaffolds for Tissue Engineering. In: NNIN REU Research Accomplishments. pp. 32–33 (2010)

32. Takeuchi, S.: Cell-laden hydrogel beads, fibers and plates for 3D tissue construction. In: 17th International Conference on Solid-State Sensors, Actuators and Microsystems, Transducers and Eurosensors, Barcelona, Spain (2013). doi:https://doi.org/10.1109/Transducers.2013.6627069

33. Young, D.A., Christman, K.L.: Injectable biomaterials for adipose tissue engineering. Biomed. Mater. **7**, 24104 (2012). https://doi.org/10.1088/1748-6041/7/2/024104

34. Lee, D.A., Reisler, T., Bader, D.L.: Expansion of chondrocytes for tissue engineering in alginate beads enhances chondrocytic phenotype compared to conventional monolayer techniques. Acta Orthop. Scand. **74**, 6–15 (2003). https://doi.org/10.1080/00016470310013581

35. Yan, S., Wang, T., Li, X., Jian, Y., Zhang, K., Li, G., Yin, J.: Fabrication of injectable hydrogels based on poly(l-glutamic acid) and chitosan. RSC Adv. **7**, 17005–17019 (2017). https://doi.org/10.1039/C7RA01864A

36. Xue, B., Kozlovskaya, V., Kharlampieva, E.: Shaped stimuli-responsive hydrogel particles: syntheses, properties and biological responses. J. Mater. Chem. B **5**, 9–35 (2017). https://doi.org/10.1039/C6TB02746F

37. El-Sherbiny, I., Yacoub, M.: Hydrogel scaffolds for tissue engineering: progress and challenges. Glob. Cardiol. Sci. Pract. **2013**, 316–342 (2013). https://doi.org/10.5339/gcsp.2013.38

38. Teixeira, S., Fernandes, H., Leusink, A., Van Blitterswijk, C., Ferraz, M.P., Monteiro, F.J., De Boer, J.: In vivo evaluation of highly macroporous ceramic scaffolds for bone tissue engineering. J. Biomed. Mater. Res. Part A. **93**, 567–575 (2010). https://doi.org/10.1002/jbm.a.32532

39. Blanco, J.F., Sánchez-Guijo, F.M., Carrancio, S., Muntion, S., García-Briñon, J., del Cañizo, M.C.: Titanium and tantalum as mesenchymal stem cell scaffolds for spinal fusion: an in vitro comparative study. Eur. Spine J. **20**, 1–8 (2011). https://doi.org/10.1007/s00586-011-1901-8

40. Wise, J.K., Yarin, A.L., Megaridis, C.M., Cho, M.: Chondrogenic differentiation of human mesenchymal stem cells on oriented nanofibrous scaffolds: engineering the superficial zone of articular cartilage. Tissue Eng. Part A. **15**, 913–921 (2009). https://doi.org/10.1089/ten.tea.2008.0109

41. Awaji, H., Matsunaga, T., Choi, S.-M.: Relation between strength, fracture toughness, and critical frontal process zone size in ceramics. Mater. Trans. **47**, 1532–1539 (2006). https://doi.org/10.2320/matertrans.47.1532

42. Sadiasa, A., Nguyen, T.H., Lee, B.-T.: In vitro and in vivo evaluation of porous PCL-PLLA 3D polymer scaffolds fabricated via salt leaching method for bone tissue engineering applications. J. Biomater. Sci. Polym. Ed. **25**, 150–167 (2014). https://doi.org/10.1080/09205063.2013.846633

43. Baker, S.C., Rohman, G., Southgate, J., Cameron, N.R.: The relationship between the mechanical properties and cell behaviour on PLGA and PCL scaffolds for bladder tissue engineering. Biomaterials **30**, 1321–1328 (2009). https://doi.org/10.1016/j.biomaterials.2008.11.033

44. Asran, A.S., Razghandi, K., Aggarwal, N.H.M.G., Groth, T.: Nanofibers from blends of polyvinyl alcohol and polyhydroxy butyrate as a potensional scaffold materail.pdf. Biomacromolecules **11**, 3413–3421 (2010)

45. Siparsky, G.L., Voorhees, K.J., Miao, F.: Hydrolysis of Polylactic acid (PLA) and Polycaprolactone (PCL) in aqueous Acetonitrile solutions: autocatalysis. J. Environ. Polym. Degrad. **6**, 31–41 (1998). https://doi.org/10.1023/A:1022826528673

46. Barbanti, S.H., Carvalho Zavaglia, C.A., De Rezende Duek, E.A.: Effect of salt leaching on PCL and PLGA (50/50) resorbable scaffolds 2. Material and Methods. Mater. Res. **11**, 75–80 (2008). https://doi.org/10.1590/S1516-14392008000100014

47. Sung, H.-J., Meredith, C., Johnson, C., Galis, Z.S.: The effect of scaffold degradation rate on three-dimensional cell growth and angiogenesis. Biomaterials **25**, 5735–5742 (2004). https://doi.org/10.1016/j.biomaterials.2004.01.066

48. An, J., Leeuwenburgh, S.C.G., Wolke, J.G.C., Jansen, J.A.: Effects of stirring and fluid perfusion on the in vitro degradation of calcium phosphate cement/PLGA composites. Tissue Eng. Part C. **21**, 1171–1177 (2015). https://doi.org/10.1089/ten.tec.2015.0016

49. Loh, Q.L., Choong, C.: Three-dimensional scaffolds for tissue engineering applications: role of porosity and pore size. Tissue Eng. Part B. Rev. **19**, 485–502 (2013). https://doi.org/10.1089/ten.TEB.2012.0437

50. Pulikkot, S., Greish, Y.E., Mourad, A.H.I., Karam, S.M.: Establishment of a three-dimensional culture system of gastric stem cells supporting mucous cell differentiation using microfibrous polycaprolactone scaffolds. Cell Prolif. **47**, 553–563 (2014). https://doi.org/10.1111/cpr.12141

51. Emma Campiglio, C., Marcolin, C., Draghi, L.: Electrospun ECM macromolecules as biomimetic scaffold for regenerative medicine: challenges for preserving conformation and bioactivity. AIMS Mater. Sci. **4**, 638–669 (2017). https://doi.org/10.3934/matersci.2017.3.638

52. Wendorff, J.H., Agarwal, S., Greiner, A.: Materials, Processing, and Applications. Wiley-VCH Verlag GmbH & Co., Weinheim, Germany (2012)

53. Bye, F.J., Wang, L., Bullock, A.J., Blackwood, K.A., Ryan, A.J., MacNeil, S.: Postproduction processing of electrospun fibres for tissue engineering. J. Vis. Exp. (2012). https://doi.org/10.3791/4172

54. Moon, S., Gil, M., Lee, K.J.: Syringeless electrospinning toward versatile fabrication of nanofiber web. Sci. Rep. **7**, 41424 (2017). https://doi.org/10.1038/srep41424

55. Niu, H., Lin, T.: Fiber generators in needleless electrospinning. J. Nanomater. **2012**, 1–13 (2012). https://doi.org/10.1155/2012/725950

56. Kwon, S.-M., Kim, Y.-J., Hong, J.K., Bang, J.Y., Xu, G., Lee, J.-H., Lee, H.-J., Kim, H.S.: Thickness-controllable electrospun fibers promote tubular structure formation by endothelial progenitor cells. Int. J. Nanomedicine **10**, 1189–1200 (2015). https://doi.org/10.2147/IJN.S73096

57. Aghajanpoor, M., Hashemi-Najafabadi, S., Baghaban-Eslaminejad, M., Bagheri, F., Mohammad Mousavi, S., Azam Sayyahpour, F.: The effect of increasing the pore size of nanofibrous scaffolds on the osteogenic cell culture using a combination of sacrificial agent electrospinning and ultrasonication. J. Biomed. Mater. Res. Part A. **105**, 1887–1899 (2017). https://doi.org/10.1002/jbm.a.36052

58. Vaquette, C., Cooper-White, J.J.: Increasing electrospun scaffold pore size with tailored collectors for improved cell penetration. Acta Biomater. **7**, 2544–2557 (2011). https://doi.org/10.1016/j.actbio.2011.02.036

59. Pham, Q.P., Sharma, U., Mikos, A.G.: Electrospun poly(ε-caprolactone) microfiber and multilayer nanofiber/microfiber scaffolds: characterization of scaffolds and measurement of cellular infiltration. Biomacromolecules **7**, 2796–2805 (2006). https://doi.org/10.1021/bm060680j

60. Phipps, M.C., Clem, W.C., Catledge, S.A., Xu, Y., Hennessy, K.M., Thomas, V., Jablonsky, M.J., Chowdhury, S., Stanishevsky, A.V., Vohra, Y.K., Bellis, S.L.: Mesenchymal stem cell responses to bone-mimetic electrospun matrices composed of polycaprolactone, collagen I and nanoparticulate hydroxyapatite. PLoS One **6**, 1–8 (2011). https://doi.org/10.1371/journal.pone.0016813

61. Francis, M.P., Moghaddam-White, Y.M., Sachs, P.C., Beckman, M.J., Chen, S.M., Bowlin, G.L., Elmore, L.W., Holt, S.E.: Modeling early stage bone regeneration with biomimetic electrospun fibrinogen nanofibers and adipose-derived mesenchymal stem cells. Electrospinning **1**, 10–19 (2016). https://doi.org/10.1515/esp-2016-0002

62. Yao, Q., Cosme, J.G.L., Xu, T., Miszuk, J.M., Picciani, P.H.S., Fong, H., Sun, H.: Three-dimensional electrospun PCL/PLA blend nanofibrous scaffolds with significantly improved stem cells osteogenic differentiation and cranial bone formation. Biomaterials **115**, 115–127 (2017). https://doi.org/10.1016/j.biomaterials.2016.11.018

63. Chen, H., Peng, Y., Wu, S., Tan, L.P.: Electrospun 3D fibrous scaffolds for chronic wound repair. Materials (Basel). **9**(1–12), (2016). https://doi.org/10.3390/ma9040272

64. Fazili, A., Gholami, S., Zangi, B.M., Seyedjafari, E., Gholami, M.: In vivo differentiation of mesenchymal stem cells into insulin producing cells on electrospun poly-L-Lactide acid scaffolds coated with Matricaria chamomilla L. Oil. Cell J. **18**, 310–321 (2016)

65. Silva, S.Y., Rueda, L.C., López, M., Vélez, I.D., Rueda-Clausen, C.F., Smith, D.J., Muñoz, G., Mosquera, H., Silva, F.A., Buitrago, A., Díaz, H., López-Jaramillo, P.: Double-blind, randomized controlled trial, to evaluate the effectiveness of a controlled nitric oxide releasing patch versus meglumine antimoniate in the treatment of cutaneous leishmaniasis [NCT00317629]. Trials **7**, 14 (2006). https://doi.org/10.1186/1745-6215-7-14

66. Silva, S.Y., Rueda, L.C., Márquez, G.A., López, M., Smith, D.J., Calderón, C.A., Castillo, J.C., Matute, J., Rueda-Clausen, C.F., Orduz, A., Silva, F.A., Kampeerapappun, P., Bhide, M., López-Jaramillo, P.: Double blind, randomized, placebo-controlled clinical trial for the treatment of diabetic foot ulcers, using a nitric oxide releasing patch: PATHON. Trials **8**, 26 (2007). https://doi.org/10.1186/1745-6215-8-26

67. Wu, X., Wang, Y., Zhu, C., Tong, X., Yang, M., Yang, L., Liu, Z., Huang, W., Wu, F., Zong, H., Li, H., He, H.: Preclinical animal study and human clinical trial data of co-electrospun poly(L-lactide-co-caprolactone) and fibrinogen mesh for anterior pelvic floor reconstruction. Int. J. Nanomedicine **11**, 389–397 (2016). https://doi.org/10.2147/IJN.S88803

68. Hutmacher, D.W., Singh, H.: Computational fluid dynamics for improved bioreactor design and 3D culture. Trends Biotechnol. **26**, 166–172 (2008). https://doi.org/10.1016/j.tibtech.2007.11.012

69. Chang, H., Wang, Y.: Cell responses to surface and architecture of tissue engineering scaffolds. In: Eberli, D. (ed.) Regenerative medicine and tissue engineering - Cells and biomaterials. pp. 569–588. InTech, Rijeka, Croatia (2011)

70. Aarvold, A., Smith, J.O., Tayton, E.R., Lanham, S.A., Chaudhuri, J.B., Turner, I.G., Oreffo, R.O.C.: The effect of porosity of a biphasic ceramic scaffold on human skeletal stem cell growth and differentiation in vivo. J. Biomed. Mater. Res. Part A. **101**, 3431–3437 (2013)

71. Gomes, M.E., Holtorf, H.L., Reis, R.L., Mikos, A.G.: Influence of the porosity of starch-based fiber mesh scaffolds on the proliferation and osteogenic differentiation of bone marrow stromal cells cultured in a flow perfusion bioreactor. Tissue Eng. **12**, 801–809 (2006). https://doi.org/10.1089/ten.2006.12.801

72. Ikeda, R., Fujioka, H., Nagura, I., Kokubu, T., Toyokawa, N., Inui, A., Makino, T., Kaneko, H., Doita, M., Kurosaka, M.: The effect of porosity and mechanical property of a synthetic polymer scaffold on repair of osteochondral defects. Int. Orthop. **33**, 821–828 (2008). https://doi.org/10.1007/s00264-008-0532-0

73. Lee, B.L.-P., Tang, Z., Wang, A., Huang, F., Yan, Z., Wang, D., Chu, J.S., Dixit, N., Yang, L., Li, S.: Synovial stem cells and their responses to the porosity of microfibrous scaffold. Acta Biomater. **9**, 7264–7275 (2013). https://doi.org/10.1016/j.actbio.2013.03.009

74. Fu, X., Wang, H.: Rapid fabrication of biomimetic nanofiber-enabled skin grafts. In: Webster, T.J. (ed.) Nanomedicine: Technologies and Applications. p. 428. Woodhead Publishing, Cambridge, UK (2012)

75. Sabree, I., Gough, J.E., Derby, B.: Mechanical properties of porous ceramic scaffolds: influence of internal dimensions. Ceram. Int. **41**, 8425–8432 (2015). https://doi.org/10.1016/j.ceramint.2015.03.044

76. Lowery, J.L., Datta, N., Rutledge, G.C.: Effect of fiber diameter, pore size and seeding method on growth of human dermal fibroblasts in electrospun poly(epsilon-caprolactone) fibrous mats. Biomaterials **31**, 491–504 (2010). https://doi.org/10.1016/j.biomaterials.2009.09.072

77. Milleret, V., Hefti, T., Hall, H., Vogel, V., Eberli, D.: Influence of the fiber diameter and surface roughness of electrospun vascular grafts on blood activation. Acta Biomater. **8**, 4349–4356 (2012). https://doi.org/10.1016/j.actbio.2012.07.032

78. Jabur, A.R., Al-Hassani, E.S., Al-Shammari, A.M., Najim, M.A., Hassan, A.A., Ahmed, A.A.: Evaluation of stem cells' growth on electrospun polycaprolactone (PCL) scaffolds used for soft tissue applications. Energy Procedia **119**, 61–71 (2017). https://doi.org/10.1016/j.egypro.2017.07.048

79. Vashaghian, M., Zandieh-Doulabi, B., Roovers, J.-P., Smit, T.H.: Electrospun matrices for pelvic floor repair: effect of fiber diameter on mechanical properties and cell behavior. Tissue Eng. Part A. **22**, 1305–1316 (2016). https://doi.org/10.1089/ten.tea.2016.0194

80. Elsayed, Y., Lekakou, C., Labeed, F., Tomlins, P.: Smooth muscle tissue engineering in crosslinked electrospun gelatin scaffolds. J. Biomed. Mater. Res. Part A. **104**, 313–321 (2016). https://doi.org/10.1002/jbm.a.35565

81. Bergmeister, H., Schreiber, C., Grasl, C., Walter, I., Plasenzotti, R., Stoiber, M., Bernhard, D., Schima, H.: Healing characteristics of electrospun polyurethane grafts with various porosities. Acta Biomater. **9**, 6032–6040 (2013). https://doi.org/10.1016/j.actbio.2012.12.009

82. Pham, Q.P., Sharma, U., Mikos, A.G.: Electrospinning of polymeric nanofibers for tissue engineering applications: a review. Tissue Eng. **12**, 60509065116001 (2006). https://doi.org/10.1089/ten.2006.12.ft-65

83. Soliman, S., Pagliari, S., Rinaldi, A., Forte, G., Fiaccavento, R., Pagliari, F., Franzese, O., Minieri, M., Di Nardo, P., Licoccia, S., Traversa, E.: Multiscale three-dimensional scaffolds for soft tissue engineering via multimodal electrospinning. Acta Biomater. **6**, 1227–1237 (2010). https://doi.org/10.1016/j.actbio.2009.10.051

84. Gluck, J.M.: Electrospun Nanofibrous Poly($\varepsilon$-Caprolactone) (PCL) Scaffolds for Liver Tissue Engineering (Master Thesis), Graduate Faculty of North Carolina State University (2007)

85. Cardwell, R.D., Dahlgren, L.A., Goldstein, A.S.: Electrospun fibre diameter, not alignment, affects mesenchymal stem cell differentiation into the tendon/ligament lineage. J. Tissue Eng. Regen. Med. **8**, 937–945 (2014). https://doi.org/10.1002/term.1589

86. Tatapudy, S., Aloisio, F., Barber, D., Nystul, T.: Cell fate decisions: emerging roles for metabolic signals and cell morphology. EMBO Rep. **18**, 2105–2118 (2017). https://doi.org/10.15252/embr.201744816

87. Aghamohseni, H., Ohadi, K., Spearman, M., Krahn, N., Moo-young, M., Scharer, J.M., Butler, M., Budman, H.M.: Effects of nutrient levels and average culture pH on the glycosylation pattern of camelid-humanized monoclonal antibody. J. Biotechnol. **186**, 98–109 (2014). https://doi.org/10.1016/j.jbiotec.2014.05.024

88. Monfoulet, L.-E., Becquart, P., Marchat, D., Vandamme, K., Bourguignon, M., Pacard, E., Viateau, V., Petite, H., Logeart-Avramoglou, D.: The pH in the microenvironment of human mesenchymal stem cells is a critical factor for optimal osteogenesis in tissue-engineered constructs. Tissue Eng. Part A. **20**, 1827–1840 (2014). https://doi.org/10.1089/ten.tea.2013.0500

89. Ham, R.G., Mckeehan, W.L.: Media and growth requirements. In: Jakoby, W.B., Pastan, I.H. (eds.) Methods in Enzymology Vol. 58: Cell Culture, pp. 47–93. Academic Press, New York (1979)

90. Sivakumar, S., Daum, J.R., Gorbsky, G.J.: Live-cell fluorescence imaging for phenotypic analysis of mitosis. In: Noguchi, E., Gadaleta, M. (eds.) Cell Cycle Control Vol. 1170: Methods in Molecular Biology (Methods and Protocols), pp. 549–562. Humana Press, New York, NY (2014)

91. Negoro, K., Kobayashi, S., Takeno, K., Uchida, K., Baba, H.: Effect of osmolarity on glycosaminoglycan production and cell metabolism of articular chondrocyte under three-dimensional culture system. Clin. Exp. Rheumatol. **26**, 534–541 (2008)

92. Potočar, U., Hudoklin, S., Kreft, M.E., Završnik, J., Božikov, K., Fröhlich, M.: Adipose-derived stem cells respond to increased osmolarities. PLoS One **11**, e0163870 (2016). https://doi.org/10.1371/journal.pone.0163870

93. Koay, E.J., Athanasiou, K.A.: Hypoxic chondrogenic differentiation of human embryonic stem cells enhances cartilage protein synthesis and biomechanical functionality. Osteoarthr. Cartil. **16**, 1450–1456 (2008). https://doi.org/10.1016/j.joca.2008.04.007

94. Ma, T., Grayson, W.L., Fröhlich, M., Vunjak-Novakovic, G.: Hypoxia and stem cell-based engineering of mesenchymal tissues. Biotechnol. Prog. **25**, 32–42 (2009). https://doi.org/10.1002/btpr.128

95. Dos Santos, F., Andrade, P.Z., Boura, J.S., Abecasis, M.M., Da Silva, C.L., Cabral, J.M.S.: Ex vivo expansion of human mesenchymal stem cells: a more effective cell proliferation kinetics and metabolism under hypoxia. J. Cell. Physiol. **223**, 27–35 (2010). https://doi.org/10.1002/jcp.21987

96. Deschepper, M., Oudina, K., David, B., Myrtil, V., Collet, C., Bensidhoum, M., Logeart-Avramoglou, D., Petite, H.: Survival and function of mesenchymal stem cells (MSCs) depend on glucose to overcome exposure to long-term, severe and continuous hypoxia. J. Cell. Mol. Med. **15**, 1505–1514 (2011). https://doi.org/10.1111/j.1582-4934.2010.01138.x

97. Adesida, A.B., Mulet-sierra, A., Jomha, N.M.: Hypoxia mediated isolation and expansion enhances the chondrogenic capacity of bone marrow mesenchymal stromal cells. Stem Cell Res Ther **3**, 9 (2012). https://doi.org/10.1186/scrt100

98. Freshney, R.I., Obradovic, B., Grayson, W., Cannizzaro, C., Vunjak-Novakovic, G.: Principles of tissue culture and bioreactor design. In: Lanza, R., Langer, R., Vacanti, J. (eds.) Principles of Tissue Engineering, pp. 155–183. Academic Press, San Diego (2007)

99. Nuschke, A., Rodrigues, M., Wells, A.W., Sylakowski, K., Wells, A.: Mesenchymal stem cells/multipotent stromal cells (MSCs) are glycolytic and thus glucose is a limiting factor of in vitro models of MSC starvation. Stem Cell Res. Ther. 1–9 (2016). doi:https://doi.org/10.1186/s13287-016-0436-7

100. Machado, N.M.: Glicose e Glutamina na Proliferação e Viabilidade de Células-Tronco Dentais Humanas (Master Thesis), Universidade Federal de São Paulo (2014)

101. Heywood, H.K., Bader, D.L., Lee, D.A.: Rate of oxygen consumption by isolated articular chondrocytes is sensitive to medium glucose concentration. J. Cell. Physiol. **206**, 402–410 (2006). https://doi.org/10.1002/jcp.20491

102. Kasinskas, R.W., Venkatasubramanian, R., Forbes, N.S.: Rapid uptake of glucose and lactate, and not hypoxia, induces apoptosis in three-dimensional tumor tissue culture. Integr. Biol. (Camb). **6**, 399–410 (2014). https://doi.org/10.1039/c4ib00001c

103. Farrell, M.J., Shin, J.I., Smith, L.J., Mauck, R.L.: Functional consequences of glucose and oxygen deprivation on engineered mesenchymal stem cell-based cartilage constructs. Osteoarthr. Cartil. **23**, 134–142 (2015). https://doi.org/10.1016/j.joca.2014.09.012

104. Zhang, B., Liu, N., Shi, H., Wu, H., Gao, Y., He, H., Gu, B., Liu, H.: High-glucose microenvironments inhibit the proliferation and migration of bone mesenchymal stem cells by activating GSK3β. J. Bone Miner. Metab. **34**, 140–150 (2016). https://doi.org/10.1007/s00774-015-0662-6

105. Rogatzki, M.J., Ferguson, B.S., Goodwin, M.L., Gladden, L.B.: Lactate is always the end product of glycolysis. Front. Neurosci. **9**, 1–7 (2015). https://doi.org/10.3389/fnins.2015.00022

106. Schop, D., Janssen, F.W., van Rijn, L.D.S., Fernandes, H., Bloem, R.M., de Bruijn, J.D., van Dijkhuizen-Radersma, R.: Growth, metabolism, and growth inhibitors of mesenchymal stem cells. Tissue Eng. Part A. **15**, 1877–1886 (2009). https://doi.org/10.1089/ten.tea.2008.0345

107. Chen, T., Zhou, Y., Tan, W.: Effects of low temperature and lactate on osteogenic differentiation of human amniotic mesenchymal stem cells. Biotechnol. Bioprocess Eng. **14**, 708–715 (2009). https://doi.org/10.1007/s12257-009-0034-y

108. Rödling, L., Schwedhelm, I., Kraus, S., Bieback, K., Hansmann, J., Lee-Thedieck, C.: 3D models of the hematopoietic stem cell niche under steady-state and active conditions. Sci. Rep. **7**, 4625 (2017). https://doi.org/10.1038/s41598-017-04808-0

109. Burdick, J A, Vunjak-Novakovic, G.: Engineered microenvironments for controlled stem cell differentiation. Tissue Eng. Part A. 15, 205–219 (2009). doi:https://doi.org/10.1089/ten.tea.2008.0131

110. Ferrari, C., Olmos, E., Balandras, F., Tran, N., Chevalot, I., Guedon, E., Marc, A.: Investigation of growth conditions for the expansion of porcine mesenchymal stem cells on microcarriers in stirred cultures. Appl. Biochem. Biotechnol. **172**, 1004–1017 (2014). https://doi.org/10.1007/s12010-013-0586-3

111. Sart, S., Errachid, A., Schneider, Y.-J., Agathos, S.N.: Modulation of mesenchymal stem cell actin organization on conventional microcarriers for proliferation and differentiation in stirred bioreactors. J. Tissue Eng. Regen. Med. **7**, 537–551 (2013). https://doi.org/10.1002/term.545

112. Mizukami, A., Fernandes-Platzgummer, A., Carmelo, J.G., Swiech, K., Covas, D.T., Cabral, J.M.S., da Silva, C.L.: Stirred tank bioreactor culture combined with serum−/xenogeneic-free culture medium enables an efficient expansion of umbilical cord-derived mesenchymal stem/stromal cells. Biotechnol. J. **11**, 1048–1059 (2016). https://doi.org/10.1002/biot.201500532

113. Rosa, F., Sales, K.C., Carmelo, J.G., Fernandes-Platzgummer, A., da Silva, C.L., Lopes, M.B., Calado, C.R.C.: Monitoring the ex-vivo expansion of human mesenchymal stem/stromal cells in xeno-free microcarrier-based reactor systems by MIR spectroscopy. Biotechnol. Prog. **32**, 447–455 (2016). https://doi.org/10.1002/btpr.2215

114. Grein, T.A., Leber, J., Blumenstock, M., Petry, F., Weidner, T., Salzig, D., Czermak, P.: Multiphase mixing characteristics in a microcarrier-based stirred tank bioreactor suitable for human mesenchymal stem cell expansion. Process Biochem. **51**, 1109–1119 (2016). https://doi.org/10.1016/j.procbio.2016.05.010

115. Wu, X., Li, S., Lou, L., Chen, Z.: The effect of the microgravity rotating culture system on the chondrogenic differentiation of bone marrow mesenchymal stem cells. Mol. Biotechnol. **54**, 331–336 (2013). https://doi.org/10.1007/s12033-012-9568-x

116. Bancroft, G.N., Sikavitsas, V.I., Mikos, A.G.: Design of a flow perfusion bioreactor system for bone tissue-engineering applications. Tissue Eng. **9**, 549–554 (2003). https://doi.org/10.1089/107632703322066723

117. Yeatts, A.B., Tubular perfusion system bioreactor for the dynamic culture of human mesenchymal stem cells (PhD Thesis), College Park (2012)

118. Cartmell, S.H., Porter, B.D., García, A.J., Guldberg, R.E.: Effects of medium perfusion rate on cell-seeded three-dimensional bone constructs in vitro. Tissue Eng. **9**, 1197–1203 (2003). https://doi.org/10.1089/10763270360728107

119. de Peppo, G.M., Sladkova, M., Sjövall, P., Palmquist, A., Oudina, K., Hyllner, J., Thomsen, P., Petite, H., Karlsson, C.: Human embryonic stem cell-derived mesodermal progenitors display substantially increased tissue formation compared to human mesenchymal stem cells under dynamic culture conditions in a packed bed/column bioreactor. Tissue Eng. Part A. **19**, 175–187 (2013). https://doi.org/10.1089/ten.tea.2011.0412

120. Ban, Y., Wu, Y., Yu, T., Geng, N., Wang, Y., Liu, X., Gong, P.: Response of osteoblasts to low fluid shear stress is time dependent. Tissue Cell. **43**, 311–317 (2011). https://doi.org/10.1016/j.tice.2011.06.003

121. Markhoff, J., Wieding, J., Weissmann, V., Pasold, J., Jonitz-Heincke, A., Bader, R.: Influence of different three-dimensional open porous titanium scaffold designs on human osteoblasts behavior in static and dynamic cell investigations. Materials (Basel). **8**, 5490–5507 (2015). https://doi.org/10.3390/ma8085259

122. Yang, Z., Tang, Y., Li, J., Zhang, Y., Hu, X.: Facile synthesis of tetragonal columnar-shaped $TiO_2$ nanorods for the construction of sensitive electrochemical glucose biosensor. Biosens. Bioelectron. **54**, 528–533 (2014). https://doi.org/10.1016/j.bios.2013.11.043

123. Zhang, Z., Yuan, L., Lee, P.D., Jones, E., Jones, J.R.: Modeling of time-dependent localized flow shear stress and its impact on cellular growth within additive manufactured titanium implants. J. Biomed. Mater. Res. Part B Appl. Biomater. **102**, 1689–1699 (2014). https://doi.org/10.1002/jbm.b.33146

124. Moore, M., Moore, R., McFetridge, P.S.: Directed oxygen gradients initiate a robust early remodeling response in engineered vascular grafts. Tissue Eng. Part A. **19**, 2005–2013 (2013). https://doi.org/10.1089/ten.TEA.2012.0592

125. Janssen, F.W., Oostra, J., Van Oorschot, A., Van Blitterswijk, C.A.: A perfusion bioreactor system capable of producing clinically relevant volumes of tissue-engineered bone: In vivo bone formation showing proof of concept. Biomaterials **27**, 315–323 (2006). https://doi.org/10.1016/j.biomaterials.2005.07.044

126. Liao, J., Guo, X., Grande-Allen, K.J., Kasper, F.K., Mikos, A.G.: Bioactive polymer/extracellular matrix scaffolds fabricated with a flow perfusion bioreactor for cartilage tissue engineering. Biomaterials **31**, 8911–8920 (2010). https://doi.org/10.1016/j.biomaterials.2010.07.110

127. Thibault, R.A., Mikos, A.G., Kasper, F.K.: Protein and mineral composition of osteogenic extracellular matrix constructs generated with a flow perfusion bioreactor. Biomacromolecules **12**, 4204–4212 (2011). https://doi.org/10.1021/bm200975a

128. Alves da Silva, M.L., Martins, A., Costa-Pinto, A.R., Costa, P., Faria, S., Gomes, M., Reis, R.L., Neves, N.M.: Cartilage tissue engineering using electrospun PCL nanofiber meshes and MSCs. Biomacromolecules **11**, 3228–3236 (2010). https://doi.org/10.1021/bm100476r

129. Gugerell, A., Neumann, A., Kober, J., Tammaro, L., Hoch, E., Schnabelrauch, M., Kamolz, L., Kasper, C., Keck, M.: Adipose-derived stem cells cultivated on electrospun L-lactide/glycolide copolymer fleece and gelatin hydrogels under flow conditions – aiming physiological reality in hypodermis tissue engineering. Burns **41**, 163–171 (2015). https://doi.org/10.1016/j.burns.2014.06.010

130. Weyand, B., Kasper, C., Israelowitz, M., Gille, C., von Schroeder, H.P., Reimers, K., Vogt, P.M.: A differential pressure laminar flow reactor supports osteogenic differentiation and extracellular matrix formation from adipose mesenchymal stem cells in a macroporous ceramic scaffold. Biores. Open Access **1**, 145–156 (2012). https://doi.org/10.1089/biores.2012.9901

131. Tsai, A.-C., Liu, Y., Ma, T.: Expansion of human mesenchymal stem cells in fibrous bed bioreactor. Biochem. Eng. J. **108**, 51–57 (2016). https://doi.org/10.1016/j.bej.2015.09.002

132. Yeatts, A.B., Both, S.K., Yang, W., Alghamdi, H.S., Yang, F., Fisher, J.P., Jansen, J.A.: In vivo bone regeneration using tubular perfusion system bioreactor cultured nanofibrous scaffolds. Tissue Eng. Part A. **20**, 139–146 (2014). https://doi.org/10.1089/ten.tea.2013.0168

133. Kim, J., Ma, T.: Regulation of autocrine fibroblast growth factor-2 signaling by perfusion flow in 3D human mesenchymal stem cell constructs. Biotechnol. Prog. **28**, 1384–1388 (2012). https://doi.org/10.1002/btpr.1604

134. Grayson, W.L., Marolt, D., Bhumiratana, S., Fröhlich, M., Guo, X.E., Vunjak-Novakovic, G.: Optimizing the medium perfusion rate in bone tissue engineering bioreactors. Biotechnol. Bioeng. **108**, 1159–1170 (2011). https://doi.org/10.1002/bit.23024

135. Dahlin, R.L., Meretoja, V.V., Ni, M., Kasper, F.K., Mikos, A.G.: Design of a high-throughput flow perfusion bioreactor system for tissue engineering. Tissue Eng. Part C Methods. **18**, 817–820 (2012). https://doi.org/10.1089/ten.tec.2012.0037

136. Santoro, M., Lamhamedi-Cherradi, S.-E., Menegaz, B.A., Ludwig, J.A., Mikos, A.G.: Flow perfusion effects on three-dimensional culture and drug sensitivity of Ewing sarcoma. Proc. Natl. Acad. Sci. **112**, 10304–10309 (2015). https://doi.org/10.1073/pnas.1506684112

137. Diederichs, S., Röker, S., Marten, D., Peterbauer, A., Scheper, T., van Griensven, M., Kasper, C.: Dynamic cultivation of human mesenchymal stem cells in a rotating bed bioreactor system based on the Z®RP platform. Biotechnol. Prog. **25**, 1762–1771 (2009). https://doi.org/10.1002/btpr.258

138. Neumann, A., Lavrentieva, A., Heilkenbrinker, A., Loenne, M., Kasper, C.: Characterization and application of a disposable rotating bed bioreactor for mesenchymal stem cell expansion. Bioengineering **1**, 231–245 (2014). https://doi.org/10.3390/bioengineering1040231

139. Stefani, I., Asnaghi, M.A., Cooper-White, J.J., Mantero, S.: A double chamber rotating bioreactor for enhanced tubular tissue generation from human mesenchymal stem cells. J. Tissue Eng. Regen. Med. (2017). https://doi.org/10.1002/term.2341

140. De Napoli, I.E., Scaglione, S., Giannoni, P., Quarto, R., Catapano, G.: Mesenchymal stem cell culture in convection-enhanced hollow fibre membrane bioreactors for bone tissue engineering. J. Memb. Sci. **379**, 341–352 (2011). https://doi.org/10.1016/j.memsci.2011.06.001

141. Li, S., Liu, Y., Zhou, Q., Lue, R., Song, L., Dong, S.-W., Guo, P., Kopjar, B.: A novel axial-stress bioreactor system combined with a substance exchanger for tissue engineering of 3D constructs. Tissue Eng. Part C. Methods. **20**, 205–214 (2014). https://doi.org/10.1089/ten.TEC.2013.0173

142. Holy, C.E., Shoichet, M.S., Davies, J.E.: Engineering three-dimensional bone tissue in vitro using biodegradable scaffolds: investigating initial cell-seeding density and culture period. J. Biomed. Mater. Res. **51**, 376–382 (2000). https://doi.org/10.1002/1097

143. Griffon, D.J., Abulencia, J.P., Ragetly, G.R., Fredericks, L.P., Chaieb, S.: A comparative study of seeding techniques and three-dimensional matrices for mesenchymal cell attachment. J. Tissue Eng. Regen. Med. **5**, 169–179 (2011). https://doi.org/10.1002/term.302

144. Yamanaka, K., Yamamoto, K., Sakai, Y., Suda, Y., Shigemitsu, Y., Kaneko, T., Kato, K., Kumagai, T., Kato, Y.: Seeding of mesenchymal stem cells into inner part of interconnected porous biodegradable scaffold by a new method with a filter paper. Dent. Mater. J. **34**, 78–85 (2015). https://doi.org/10.4012/dmj.2013-330

145. Solchaga, L.A., Tognana, E., Penick, K., Baskaran, H., Goldberg, V.M., Caplan, A.I., Welter, J.F.: A rapid seeding technique for the assembly of large cell/scaffold composite constructs. Tissue Eng. **12**, 1851–1863 (2006). https://doi.org/10.1089/ten.2006.12.1851

146. Godbey, W.T., Stacey Hindy, B.S., Sherman, M.E., Atala, A.: A novel use of centrifugal force for cell seeding into porous scaffolds. Biomaterials **25**, 2799–2805 (2004). https://doi.org/10.1016/j.biomaterials.2003.09.056

147. Ng, R., Gurm, J.S., Yang, S.-T.: Centrifugal seeding of mammalian cells in nonwoven fibrous matrices. Biotechnol. Prog. 26, n/a-n/a (2009). doi:https://doi.org/10.1002/btpr.317

148. Buizer, A.T., Veldhuizen, A.G., Bulstra, S.K., Kuijer, R.: Static versus vacuum cell seeding on high and low porosity ceramic scaffolds. J. Biomater. Appl. **29**, 3–13 (2014). https://doi.org/10.1177/0885328213512171

149. Wanasekara, N.D., Ghosh, S., Chen, M., Chalivendra, V.B., Bhowmick, S.: Effect of stiffness of micron/sub-micron electrospun fibers in cell seeding. J. Biomed. Mater. Res. Part A. **103**, 2289–2299 (2015). https://doi.org/10.1002/jbm.a.35362

150. Fu, W.-J., Xu, Y.-D., Wang, Z.-X., Li, G., Shi, J.-G., Cui, F.-Z., Zhang, Y., Zhang, X.: New ureteral scaffold constructed with composite poly(L-lactic acid)-collagen and urothelial cells by new centrifugal seeding system. J. Biomed. Mater. Res. Part A. **100A**, 1725–1733 (2012). https://doi.org/10.1002/jbm.a.34134

151. Kim, B.-S., Putnam, A.J., Kulik, T.J., Mooney, D.J.: Optimizing seeding and culture methods to engineer smooth muscle tissue on biodegradable polymer matrices. Biotechnol. Bioeng. **57**, 46–54 (1998). https://doi.org/10.1002/(SICI)1097-0290(19980105)57:1<46::AID-BIT6>3.0.CO;2-V

152. Wendt, D., Marsano, A., Jakob, M., Heberer, M., Martin, I.: Oscillating perfusion of cell suspensions through three-dimensional scaffolds enhances cell seeding efficiency and uniformity. Biotechnol. Bioeng. **84**, 205–214 (2003). https://doi.org/10.1002/bit.10759

153. Zhao, F., Ma, T.: Perfusion bioreactor system for human mesenchymal stem cell tissue engineering: dynamic cell seeding and construct development. Biotechnol. Bioeng. **91**, 482–493 (2005). https://doi.org/10.1002/bit.20532

154. Ajalloueian, F., Lim, M.L., Lemon, G., Haag, J.C., Gustafsson, Y., Sjöqvist, S., Beltrán-Rodríguez, A., Del Gaudio, C., Baiguera, S., Bianco, A., Jungebluth, P., Macchiarini, P.: Biomechanical and biocompatibility characteristics of electrospun polymeric tracheal scaffolds. Biomaterials **35**, 5307–5315 (2014). https://doi.org/10.1016/j.biomaterials.2014.03.015

155. Ladd, M.R., Hill, T.K., Yoo, J.J., Lee, S.J.: Electrospun Nanofibers. In: Lin, T. (ed.) Tissue Engineering, Nanofibers - Production, Properties and Functional Applications. InTech (2011)

156. Barker, D.A., Bowers, D.T., Hughley, B., Chance, E.W., Klembczyk, K.J., Brayman, K.L., Park, S.S., Botchwey, E.: A: multilayer cell-seeded polymer nanofiber constructs for soft-tissue reconstruction. JAMA Otolaryngol. Head Neck Surg. **139**, 914–922 (2013). https://doi.org/10.1001/jamaoto.2013.4119

157. Dunn, J.C.Y., Chan, W.-Y., Cristini, V., Kim, J.S., Lowengrub, J., Singh, S., Wu, B.M.: Analysis of cell growth in three-dimensional scaffolds. Tissue Eng. **12**, 705–716 (2006). https://doi.org/10.1089/ten.2006.12.705

158. Papenburg, B.J., Liu, J., Higuera, G.A., Barradas, A.M.C., de Boer, J., van Blitterswijk, C.A., Wessling, M., Stamatialis, D.: Development and analysis of multi-layer scaffolds for tissue engineering. Biomaterials **30**, 6228–6239 (2009). https://doi.org/10.1016/j.biomaterials.2009.07.057

159. Srouji, S., Kizhner, T., Suss-Tobi, E., Livne, E., Zussman, E.: 3-D Nanofibrous electrospun multilayered construct is an alternative ECM mimicking scaffold. J. Mater. Sci. Mater. Med. **19**, 1249–1255 (2008). https://doi.org/10.1007/s10856-007-3218-z

160. Gugerell, A., Neumann, A., Kober, J., Tammaro, L., Hoch, E., Schnabelrauch, M., Kamolz, L., Kasper, C., Keck, M.: Adipose-derived stem cells cultivated on electrospun l-lactide/glycolide copolymer fleece and gelatin hydrogels under flow conditions – aiming physiological reality in hypodermis tissue engineering. Burns **41**, 163–171 (2014). https://doi.org/10.1016/j.burns.2014.06.010

161. Ardakani, A.G., Cheema, U., Brown, R.A., Shipley, R.J.: Quantifying the correlation between spatially defined oxygen gradients and cell fate in an engineered three-dimensional culture model. J. R. Soc. Interface **11**, 20140501–20140501 (2014). https://doi.org/10.1098/rsif.2014.0501

162. Coletti, F., Macchietto, S., Elvassore, N.: Mathematical modeling of three-dimensional cell cultures in perfusion bioreactors. Ind. Eng. Chem. Res. **45**, 8158–8169 (2006). https://doi.org/10.1021/ie051144v

163. Decuzzi, P., Ferrari, M.: Modulating cellular adhesion through nanotopography. Biomaterials **31**, 173–179 (2010). https://doi.org/10.1016/j.biomaterials.2009.09.018

164. Gómez-Pachón, E.Y., Sánchez-Arévalo, F.M., Sabina, F.J., Maciel-Cerda, A., Campos, R.M., Batina, N., Morales-Reyes, I., Vera-Graziano, R.: Characterisation and modelling of the elastic properties of poly(lactic acid) nanofibre scaffolds. J. Mater. Sci. **48**, 8308–8319 (2013). https://doi.org/10.1007/s10853-013-7644-7

165. Jungreuthmayer, C., Jaasma, M.J., Al-Munajjed, A.A., Zanghellini, J., Kelly, D.J., O'Brien, F.J.: Deformation simulation of cells seeded on a collagen-GAG scaffold in a flow perfusion bioreactor using a sequential 3D CFD-elastostatics model. Med. Eng. Phys. **31**, 420–427 (2009). https://doi.org/10.1016/j.medengphy.2008.11.003

166. Ma, C.Y.J., Kumar, R., Xu, X.Y., Mantalaris, A.: A combined fluid dynamics, mass transport and cell growth model for a three-dimensional perfused bioreactor for tissue engineering of haematopoietic cells. Biochem. Eng. J. **35**, 1–11 (2007). https://doi.org/10.1016/j.bej.2006.11.024

167. McCoy, R.J., O'Brien, F.J.: Visualizing feasible operating ranges within tissue engineering systems using a "windows of operation" approach: a perfusion-scaffold bioreactor case study. Biotechnol. Bioeng. **109**, 3161–3171 (2012). https://doi.org/10.1002/bit.24566

168. Santamaría, V.A.A., Malvè, M., Duizabo, A., Mena Tobar, A., Gallego Ferrer, G., García Aznar, J.M., Doblaré, M., Ochoa, I.: Computational methodology to determine fluid related parameters of non regular three-dimensional scaffolds. Ann. Biomed. Eng. **41**, 2367–2380 (2013). https://doi.org/10.1007/s10439-013-0849-8

169. Truscello, S., Kerckhofs, G., Van Bael, S., Pyka, G., Schrooten, J., Van Oosterwyck, H.: Prediction of permeability of regular scaffolds for skeletal tissue engineering: a combined computational and experimental study. Acta Biomater. **8**, 1648–1658 (2012). https://doi.org/10.1016/j.actbio.2011.12.021

170. Yan, X., Bergstrom, D.J., Chen, X.B.: Modeling of cell cultures in perfusion bioreactors. IEEE Trans. Biomed. Eng. **59**, 2568–2575 (2012). https://doi.org/10.1109/TBME.2012.2206077

171. Akalp, U., Bryant, S.J., Vernerey, F.J.: Tuning tissue growth with scaffold degradation in enzyme-sensitive hydrogels: a mathematical model. Soft Matter **12**, 7505–7520 (2016). https://doi.org/10.1039/c6sm00583g

172. Chen, Y., Zhou, S., Li, Q.: Mathematical modeling of degradation for bulk-erosive polymers: Applications in tissue engineering scaffolds and drug delivery systems. Acta Biomater. **7**, 1140–1149 (2011). https://doi.org/10.1016/j.actbio.2010.09.038

173. Ferdous, J., Kolachalama, V.B., Shazly, T.: Impact of polymer structure and composition on fully resorbable endovascular scaffold performance. Acta Biomater. **9**, 6052–6061 (2013). https://doi.org/10.1016/j.actbio.2012.12.011

174. Heljak, M., Swieszkowski, W., Kurzydlowski, K.J.: A phenomenological model for the degradation of polymeric tissue engineering scaffolds. In: Proceedings of the International Conference on Computer Methods in Mechanics, Warsaw, Poland (2011)

175. Heljak, M., Swieszkowski, W., Kurzydlowski, K.J.: Modeling of the degradation kinetics of biodegradable scaffolds: the effects of the environmental conditions. J. Appl. Polym. Sci. **131**, 1–7 (2014). https://doi.org/10.1002/app.40280

176. Shazly, T., Kolachalama, V.B., Ferdous, J., Oberhauser, J.P., Hossainy, S., Edelman, E.R.: Assessment of material by-product fate from bioresorbable vascular scaffolds. Ann. Biomed. Eng. **40**, 955–965 (2012). https://doi.org/10.1007/s10439-011-0445-8

177. Devarapalli, M., Lawrence, B.J., Madihally, S.V.: Modeling nutrient consumptions in large flow-through bioreactors for tissue engineering. Biotechnol. Bioeng. **103**, 1003–1015 (2009). https://doi.org/10.1002/bit.22333

178. Hidalgo-Bastida, L.A., Thirunavukkarasu, S., Griffiths, S., Cartmell, S.H., Naire, S.: Modeling and design of optimal flow perfusion bioreactors for tissue engineering applications. Biotechnol. Bioeng. **109**, 1095–1099 (2012). https://doi.org/10.1002/bit.24368

179. Pathi, P., Ma, T., Locke, B.R.: Role of nutrient supply on cell growth in bioreactor design for tissue engineering of hematopoietic cells. Biotechnol. Bioeng. **89**, 743–758 (2005). https://doi.org/10.1002/bit.20367

180. Schirmaier, C., Jossen, V., Kaiser, S.C., Jüngerkes, F., Brill, S., Safavi-Nab, A., Siehoff, A., van den Bos, C., Eibl, D., Eibl, R.: Scale-up of adipose tissue-derived mesenchymal stem cell production in stirred single-use bioreactors under low-serum conditions. Eng. Life Sci. **14**, 292–303 (2014). https://doi.org/10.1002/elsc.201300134

181. Singh, H., Teoh, S.H., Low, H.T., Hutmacher, D.W.: Flow modelling within a scaffold under the influence of uni-axial and bi-axial bioreactor rotation. J. Biotechnol. **119**, 181–196 (2005). https://doi.org/10.1016/j.jbiotec.2005.03.021

182. Chung, C.A., Lin, T.-H., Chen, S.-D., Huang, H.-I.: Hybrid cellular automaton modeling of nutrient modulated cell growth in tissue engineering constructs. J. Theor. Biol. **262**, 267–278 (2010). https://doi.org/10.1016/j.jtbi.2009.09.031

183. Doagă, I.O., Savopol, T., Neagu, M., Neagu, A., Kovács, E.: The kinetics of cell adhesion to solid scaffolds: an experimental and theoretical approach. J. Biol. Phys. **34**, 495–509 (2008). https://doi.org/10.1007/s10867-008-9108-x

184. Jeong, D., Yun, A., Kim, J.: Mathematical model and numerical simulation of the cell growth in scaffolds. Biomech. Model. Mechanobiol. **11**, 677–688 (2012). https://doi.org/10.1007/s10237-011-0342-y

185. Campolo, M., Curcio, F., Soldati, A.: Minimal perfusion flow for osteogenic growth of mesenchymal stem cells on lattice scaffolds. AICHE J. **59**, 3131–3144 (2013). https://doi.org/10.1002/aic.14084

186. Causin, P., Sacco, R.: A computational model for biomass growth simulation in tissue engineering. Commun. Appl. Ind. Math. **2**, (2011). https://doi.org/10.1685/journal.caim.370

187. Chung, C.A., Chen, C.W., Chen, C.P., Tseng, C.S.: Enhancement of cell growth in tissue-engineering constructs under direct perfusion: modeling and simulation. Biotechnol. Bioeng. **97**, 1603–1616 (2007). https://doi.org/10.1002/bit.21378

188. Flaibani, M., Magrofuoco, E., Elvassore, N.: Computational modeling of cell growth heterogeneity in a perfused 3D scaffold. Ind. Eng. Chem. Res. **49**, 859–869 (2010). https://doi.org/10.1021/ie900418g

189. Lesman, A., Blinder, Y., Levenberg, S.: Modeling of flow-induced shear stress applied on 3D cellular scaffolds: implications for vascular tissue engineering. Biotechnol. Bioeng. **105**, 645–654 (2010). https://doi.org/10.1002/bit.22555

190. Liu, D., Chua, C.K., Leong, K.F.: A mathematical model for fluid shear-sensitive 3D tissue construct development. Biomech. Model. Mechanobiol. **12**, 19–31 (2013). https://doi.org/10.1007/s10237-012-0378-7

191. Porter, B., Zauel, R., Stockman, H., Guldberg, R., Fyhrie, D.: 3-D computational modeling of media flow through scaffolds in a perfusion bioreactor. J. Biomech. **38**, 543–549 (2005). https://doi.org/10.1016/j.jbiomech.2004.04.011

192. Raimondi, M.T., Boschetti, F., Falcone, L., Fiore, G.B., Remuzzi, A., Marinoni, E., Marazzi, M., Pietrabissa, R.: Mechanobiology of engineered cartilage cultured under a quantified fluid-dynamic environment. Biomech. Model. Mechanobiol. **1**, 69–82 (2002). https://doi.org/10.1007/s10237-002-0007-y

193. Zhao, F., Chella, R., Ma, T.: Effects of shear stress on 3-D human mesenchymal stem cell construct development in a perfusion bioreactor system: experiments and hydrodynamic modeling. Biotechnol. Bioeng. **96**, 584–595 (2007). https://doi.org/10.1002/bit.21184

194. Doagă, I.O., Savopol, T., Neagu, M., Neagu, A., Kovács, E.: The kinetics of cell adhesion to solid scaffolds: an experimental and theoretical approach. J. Biol. Phys. **34**, 495–509 (2008). https://doi.org/10.1007/s10867-008-9108-x

195. Sacco, R., Causin, P., Zunino, P., Raimondi, M.T.: A multiphysics/multiscale 2D numerical simulation of scaffold-based cartilage regeneration under interstitial perfusion in a bioreactor. Biomech. Model. Mechanobiol. **10**, 577–589 (2011). https://doi.org/10.1007/s10237-010-0257-z